Channel Distribution Learning: Model-Driven GAN-Based Channel Modeling for IRS-Aided Wireless Communication

Yi Wei, Ming-Min Zhao, *Member, IEEE*, and Min-Jian Zhao, *Senior Member, IEEE*

***Abstract*— Intelligent reflecting surface (IRS) is a promising new technology that is able to create a favorable wireless signal propagation environment by collaboratively reconfiguring the passive reflecting elements yet with low hardware and energy cost. In IRS-aided wireless communication systems, channel modeling is a fundamental task for communication algorithm design and performance optimization, which however is also very challenging since in-depth domain knowledge and technical expertise in radio signal propagations are required, especially for modeling the high-dimensional cascaded base station (BS)-IRS and IRS-user channels (also referred to as the reflected channels). In this paper, we propose a model-driven generative adversarial network (GAN)-based channel modeling framework to autonomously learn the reflected channel distribution, without complex theoretical analysis or data processing. The designed GAN (also named as IRS-GAN) is trained to reach the Nash equilibrium of a minimax game between a generative model and a discriminative model. For the single-user case, we propose to incorporate the special structure of the reflected channels into the design of the generative model. While for the multiuser case, we extend the IRS-GAN and present a multiuser IRS-GAN (abbreviated as IRS-GAN-M), where the distributions of the reflected channels associated with different users are learned simultaneously with reduced number of network parameters (as compared to the naive scheme that assigns a dedicated IRS-GAN for each user). Moreover, theoretical analysis is presented to prove that the minimax game in the IRS-GAN-M framework has a global optimum if the generative and discriminative models are given with enough capacity. Simulation results are presented to validate the effectiveness of the proposed IRS-GAN framework.**

***Index Terms*— Intelligent reflecting surface (IRS), generative adversarial network (GAN), deep learning, channel modeling, multiuser communications, multiple-output single-input (MISO).**

Manuscript received 16 December 2021; revised 3 April 2022; accepted 10 May 2022. Date of publication 19 May 2022; date of current version 15 July 2022. This work was supported in part by the National Key Research and Development Program of China under Grant 2018YFB1802303, in part by the National Natural Science Foundation of China under Grant 62001417, and in part by the Zhejiang Provincial Natural Science Foundation of China under Grant LQ20F010010. An earlier version of this paper was presented in part at the IEEE GLOBECOM 2021 [DOI: 10.1109/GLOBECOM46510.2021.9685602]. The associate editor coordinating the review of this article and approving it for publication was Z. Qin. *(Corresponding author: Ming-Min Zhao.)*

The authors are with the College of Information Science and Electronic Engineering, Zhejiang University, Hangzhou 310027, China, and also with the Zhejiang Provincial Key Laboratory of Information Processing, Communication and Networking (IPCAN), Hangzhou 310027, China (e-mail: 21731133@zju.edu.cn; zmmblack@zju.edu.cn; mjzhao@zju.edu.cn).

The Python codes for generating the network proposed in this work are available online at https://github.com/YiWei0129/IRS-GAN.

Color versions of one or more figures in this article are available at https://doi.org/10.1109/TCOMM.2022.3176316.

Digital Object Identifier 10.1109/TCOMM.2022.3176316

I. Introduction

RECENTLY, intelligent reflecting surface (IRS) has been proposed as a promising new paradigm to enhance the spectral and energy efficiency of wireless communication systems with low hardware cost and energy consumption [1]–[4]. In general, IRS is a man-made planar metasurface consisting of a large number of passive and low-cost reflecting elements, each of which can be independently adjusted to induce certain amplitude and/or phase change of the incident signal by an external controller. As a result, IRS is able to collaboratively reconfigure the wireless channel and create a favorable wireless signal propagation environment for enhanced communication. In addition, compared with the conventional half-duplex amplify-and-forward (AF) relay, IRS can intelligently adjust its reflection coefficients at different reflecting elements in an inherent full-duplex manner, while free of self-interference.

Due to the abovementioned advantages, IRS has attracted significant research attention recently and various works have been conducted in the literature to show the effectiveness of IRS in enhancing the system performance, see e.g., [5]–[8]. To reap the performance gains offered by IRS, the acquisition of the channel state information (CSI) is of significant importance, but it is a difficult task since IRS is generally not equipped with any transmit/receive radio frequency (RF) chains and thus not capable of performing complex baseband signal processing tasks. To alleviate the demand for full instantaneous CSI, some prior knowledge of the IRS-related channels, e.g., the underlying channel model or the statistical CSI, are considerably vital, which can be utilized to design advanced active and passive beamforming algorithms with reduced channel training overhead [9]–[11].

Since the wireless channels have a crucial impact on the design and practical implementation of wireless communication systems, it is of great interest and significance to study and model them. Accurate channel models can help us build and deploy feasible and efficient communication technologies that are suitable for various wireless propagation environments. In the literature, various works have been conducted to develop efficient channel modeling methods for different communication systems. Specifically, the parameter-based channel sounder is a popular channel modeling method, and it was adopted in [12] to measure a set of channel parameters such as angles of departure (AoDs), angles of arrival (AoAs) and Doppler shift, etc. These parameters are further combined to reconstruct the channel impulse response. Also, data mining

technologies can be employed to extract the hidden information embedded in the historical channel samples and thereby solve the channel modeling problem. For example, in [13], the principal components analysis (PCA) method was exploited to extract hidden features from channel data and characterize the underlying channel models. The work [14] discussed the challenges and opportunities in clustering-enabled wireless channel modeling techniques. Since the intra-cluster characteristics can often be described by statistical models with very few parameters, this kind of channel modeling methods is very efficient and compact. Furthermore, geometry-based stochastic channel models (GSCMs) [15] have been found well suited for non-stationary environments, which build on placing scatterers at random according to certain statistical distributions and assigning them (scattering) properties.

However, the abovementioned channel modeling methods usually require in-depth domain knowledge and practical experience in wireless communications, and they are generally very complex especially when a large number of unknown parameters are involved in the corresponding models. In addition, these methods are not flexible when being applied to other communication environments. Recently, deep learning (DL) techniques have been widely applied to solve wireless communication problems [16], [17]. Specifically, by interpreting the channel modeling problem as a channel distribution learning problem, DL techniques can also be regarded as promising candidates to tackle the abovementioned challenges. As a result, various DL techniques have been employed for channel distribution learning, see e.g., [18]–[21]. Specifically, in [18], the authors utilized the universal approximation capability of neural networks to predict the channel characteristics of millimetre wave (mmWave) massive multiple-input multiple-output (MIMO) channels, which include amplitude, delay, AoAs and AoDs. To circumvent complex theoretical analysis and data processing, the work [19] exploited the generative adversarial network (GAN) framework [22] for channel modeling, where the channel distributions are estimated via an adversarial process. In particular, a generative model (captures the data distribution) and a discriminative model (estimates the probability that a sample is from the training data) are trained simultaneously and they compete against each other during the training process. Furthermore, the works [20] and [21] developed end-to-end wireless communication systems using deep neural networks (DNNs), where a conditional GAN is exploited to represent the channel effects and bridge the transmitter and receiver DNNs, such that the gradients of the end-to-end loss can be back-propagated to the transmitter DNN through the conditional GAN.

In the abovementioned works, only a limited number of channel parameters of the presumed channel model or the one-dimensional channel impulse response are learned, while how to characterize the distribution of high-dimensional channel matrices is still unsolved, as in our considered case. Specially, due to the passive nature of IRS, its signal processing capability is limited and hence the BS-IRS and IRS-user channels cannot be measured independently in general. Besides, only a certain number of cascaded BS-IRS and IRS-user channel (also referred to as *reflected channel*) samples can be estimated and collected [23], [24], which makes the channel modeling task more stringent. To tackle this challenge and motivated by the recent success of applying DL techniques to solve communication problems, in this paper we interpret the channel modeling problem as a channel distribution learning problem and then propose a novel model-driven GAN-based channel modeling method to characterize the distribution of the reflected channel for an IRS-aided multiple-input single-output (MISO) communication system. Note that instead of mathematically expressing the channel models, the proposed DL-based channel modeling method learns their implicit description through training, and the generated channel samples can be further utilized for theoretical analysis, performance evaluation, algorithm design and system deployment of the communication systems as vital prior information [25]. The utilization of GAN can reduce the demand of deep domain knowledge and wireless environment information, and the proposed GAN-based channel modeling method offers a high degree of flexibility under various channel models. Moreover, different from the Monte Carlo method which estimates a probability distribution by random sampling [26], GANs are more efficient since the prior knowledge of the problem can be incorporated into the design of the network structure.

To the best of our knowledge, this is the first work on reflected channel modeling for IRS-aided communication systems and the new contributions of this paper are summarized as follows:

- First, we consider the single-user case and propose a GAN-based framework, referred to as *IRS-GAN*, which consists of a generative model and a discriminative model. The generative model is expected to learn to produce random channel samples that follow the true reflected channel distribution and the discriminative model is utilized to distinguish the true channel samples from the randomly generated channel samples produced by the generative model. The proposed framework corresponds to a minimax two-player game, where the generative and discriminative models are competing with each other during the training procedure. The trained generative model can output channel samples that are as similar as the true samples, and it can be interpreted as a channel sample generation function where the learned network parameters serve as the channel distribution parameters. It is noteworthy that training GANs is known to be difficult as the minimax game between the two models needs be carefully crafted, especially for learning high-dimensional distributions of the IRS-related channels. To simply the training of IRS-GAN, we exploit the idea of model-driven DL in this work, where the special structure of the reflected channels is taken into consideration in the generative model. Specifically, the proposed generative model is mainly composed of three nodes, i.e., a BS-IRS (BI) node, an IRS-user (IU) node and a Cascading (C) node, which are supposed to approximate the BS-IRS channel, approximate the IRS-user channel, and learn to cascade the BS-IRS and IRS-user channels, respectively. We show that the training process

of IRS-GAN can be greatly simplified by adopting this structure and in the meantime the channel modeling quality is significantly improved. Besides, considering that the reflected channel is generally spatially correlated and can be viewed as a 2D image, a convolutional neural network (CNN) is employed in the generative model due to its capability of efficient feature extraction. Similarly, in the discriminative model, CNN is also employed to extract the high-dimensional features of the reflected channels. Inspired by Wasserstein GAN (WGAN) [27], [28], we propose to use a Wasserstein distance based loss function which is able to guarantee the steady convergence of IRS-GAN. A gradient penalty term and a moment penalty term are further added to the loss function to accelerate the training process.

- Second, we consider the general multiuser case where the reflected channels associated with different users are required to be modeled. Note that in this case, simply duplicating the IRS-GAN used in the single user case multiple times is very inefficient, since the number of network parameters can be considerably large and this may lead to low training speed and high hardware cost. To reduce the number of network parameters and simplify the training process, we propose a multiuser IRS-GAN framework (referred to as *IRS-GAN-M* in the following), where the strong correlation among the reflected channels associated with different users, i.e., the IRS reflecting elements reflect the signal from the BS to different users via the same IRS-BS channel, is exploited. As such, the generative model in IRS-GAN-M consists of only one BI node, K IU nodes and K C nodes, where K is the number of users. Based on this structure, the reflected channels associated with different users can be modeled simultaneously with less network parameters as compared to the naive scheme with multiple single-user IRS-GANs. The discriminative model associated with each user is the same as the IRS-GAN in the single-user case. A novel joint loss function and a multiuser joint learning strategy are also presented. Furthermore, we prove that the minimax game between the generative model and K discriminative models in the proposed IRS-GAN-M can reach their optimum as long as they are given with enough capacity.
- Finally, extensive numerical results are presented to validate the effectiveness of the proposed IRS-GAN and IRS-GAN-M by using the channel date generated by canonical channel models and professional channel simulation software. We show that the reflected channel distributions in both single-user and multiuser cases can be learned efficiently.

The rest of this paper is organized as follows. Section II presents the considered IRS-aided MISO system model. Section III introduces the details of the proposed IRS-GAN framework for the single-user case. The IRS-GAN-M for the multiuser case, the multiuser joint learning strategy, and the corresponding optimality analysis are presented in Section IV. Numerical results are presented in Section V and finally, Section VI concludes this paper.

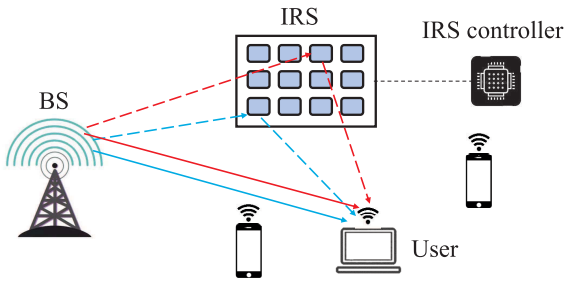

Fig. 1. An IRS-aided multiuser MISO communication system.

Notations: Scalars, vectors and matrices are respectively denoted by lower (upper) case, boldface lower case and boldface upper case letters. For a matrix $\mathbf{X}$ of arbitrary size, $\mathbf{X}^T$, $\mathbf{X}^*$, $\mathbf{X}^H$ and $[\mathbf{X}]_{m,n}$ denote the transpose, conjugate, conjugate transpose and the (m,n)-th entry of $\mathbf{X}$, respectively. The symbol $\|\cdot\|$ denotes the Euclidean norm of a complex vector, and $|\cdot|$ is the absolute value of a complex scalar; $\text{diag}(x_1,\cdots,x_N)$ denotes a diagonal matrix whose diagonal elements are set as $x_1,\cdots,x_N$. $\mathbb{C}^{m\times n}$ denotes the space of $m\times n$ complex matrices. The notation $\mathbb{E}(\cdot)$ represents the expectation of a random variable. Finally, we define the complex normal distribution with mean μ and variance σ^2 and the uniform distribution on the interval $[a,b]$ as $\mathcal{CN}(\mu,\sigma^2)$ and $U(a,b)$, respectively.

II. System Model

We consider an IRS-aided multiuser MISO system, where an N-element IRS is deployed to improve the communications from an M-antenna BS to K single-antenna users (denoted by $\{U_1,\cdots,U_K\}$) simultaneously, as shown in Fig. 1. Let $\mathbf{h}_{d,k}\in\mathbb{C}^{M\times 1}$, $\mathbf{h}_{r,k}\in\mathbb{C}^{N\times 1}$ and $\mathbf{G}\in\mathbb{C}^{N\times M}$ denote the baseband equivalent channels from the BS to U_k, from the IRS to U_k, from the BS to the IRS, respectively.

In the considered system, each reflecting element at the IRS is able to induce an independent phase-shift change of the incident signal sent by the BS. Thus, by properly adjusting the IRS reflection coefficients at different reflecting elements, a preferable wireless signal propagation environment between the transmitter and receiver can be created to enhance the communication performance. Let $\boldsymbol{\theta}\in\mathbb{C}^{N\times 1}$ denote the reflection coefficient vector where the n-th element θ_n satisfies

$$|\theta_{n,i}| = \begin{cases} 1, & \text{if element } n \text{ is on at time instant } i, \\ 0, & \text{otherwise.} \end{cases} \tag{1}$$

It is noteworthy that the proposed framework can be readily extended to the case with more practical reflection models where the amplitude and phase of each IRS element might be dependent. In this work, we consider the classical independent diffusive scatterer-based IRS model [29], which accounts for the basic properties of IRSs and is one of the most widely-adopted IRS models [5]–[9]. Specifically, by introducing an $N\times N$ diagonal reflection coefficient matrix $\boldsymbol{\Theta}=\text{diag}([\theta_1,\cdots,\theta_N])$, the received signal at U_k can be written as

$$y_k = (\mathbf{h}_{r,k}^H\boldsymbol{\Theta}\mathbf{G}+\mathbf{h}_{d,k}^H)\mathbf{x}+n_k, \tag{2}$$

where $n_k \sim \mathcal{CN}(0, \sigma^2)$ is the additive white Gaussian noise (AWGN), and $\mathbf{x} = \sum_{k=1}^{K} \mathbf{w}_k s_k$ is the complex signal transmitted by the BS with s_k and $\mathbf{w}_k$ denoting the information symbol and active precoding vector for U_k, respectively. Due to the fact that the IRS is generally not equipped with any RF chains and thus not capable of performing complex signal processing tasks, the acquisition of the BS-IRS and IRS-user channels is very difficult. To address this issue, we define the reflected channel from the BS to U_k via the IRS as

$$\mathbf{H}_k \triangleq \mathbf{G}^H \text{diag}(\mathbf{h}_{r,k}) \in \mathbb{C}^{M \times N}, \tag{3}$$

then the received signal in (2) can be equivalently rewritten as

$$y_k = (\boldsymbol{\theta}^H \mathbf{H}_k^H + \mathbf{h}_{d,k}^H)\mathbf{x} + n_k. \tag{4}$$

It can be observed that based on the knowledge of the instantaneous CSI of the BS-user and BS-IRS-user links, the active transmit precoding vectors at the BS and/or the passive phase shifts at the IRS can be separately or jointly optimized to realize the potentials of IRS-aided wireless systems, see e.g., [6], [8], [9].

To reduce the channel training overhead, the statistical CSI can be exploited as it varies much slowly as compared to the instantaneous CSI [9], [30], [31]. By efficient channel modeling, we can re-generate a large number of channel samples, and accordingly obtain the statistical CSI, e.g., the statistical mean and covariance of the channel matrices, etc. However, accurate channel modeling is very difficult, since extensive knowledge and experiences in the wireless communication field are required, especially when MIMO communication systems are considered.[1] To resolve this difficulty, we leverage the strong power of DL techniques to learn the reflected channel distribution, and accordingly propose the novel model-driven GAN-based channel modeling methods for both single-user and multiuser cases.[2]

III. IRS-GAN For Single-User System

In this section, we first introduce some preliminaries of GAN, after which we present a detailed description of the proposed IRS-GAN framework and explain the intuition behind it. Finally, we provide the learning strategy for the proposed IRS-GAN framework. Note that in this section, we only consider the single-user case for simplicity, and the extension to the general multiuser case is discussed in the next section.

A. Preliminaries of GAN

Recently, GAN has emerged as a novel framework for distribution learning via an adversarial process, which aims to learn a generative model that is able to produce samples close to some target distribution [22], [27], [28]. Different from the classical Markov chain based generative methods, such as the denoising autoencoder [33] and the generative stochastic network [34], which can only learn a blurry target distribution, GANs do not require feedback loops during generation and they can represent very sharp, and even degenerate distributions. Moreover, as compared to the variational autoencoders (VAEs) [35], which focus on learning the approximate likelihood of the samples, GANs can offer much more flexibility in the definition of the objective function. Due to these advantages, GAN-based methods have been widely utilized to learn probability distributions over various types of data, such as natural images, speech audio waveforms and symbols in natural language corpora, etc.

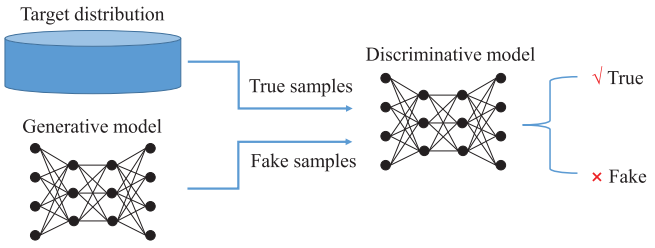

Fig. 2. Architecture of GANs.

As shown in Fig. 2, a typical GAN generally consists of a generative model and a discriminative model. These two models are trained simultaneously, and they are competing with each other in the training stage. The discriminative model is trained to distinguish the true samples from the target distribution and the fake samples generated by the generative model, while the generative model learns to fool the discriminative model into making mistakes. This framework corresponds to a minimax two-player game, and the training process will end up with a Nash equilibrium, where the discriminative model cannot outperform random guessing when distinguishing the true and fake samples. In [22], it was demonstrated that this minimax game has a global optimum, and GANs can accurately recover the target distribution as long as the generative and discriminative models have enough capacity.

Nevertheless, despite the abovementioned strengths of GANs, training them is known for being delicate and unstable, and hence it is difficult to ensure their convergence [22], [27]. Another problem is that the trained generative model may be lack of diversity, i.e., the generative model may concentrate on samples that only exhibit a few patterns instead of from the whole data space.

B. Proposed IRS-GAN Framework

In this subsection, we present the proposed IRS-GAN framework, where a specially designed GAN that takes the structure of the cascaded BS-IRS-user channel into consideration is applied to learn the channel distribution. The proposed framework consists of a generative model $\mathcal{F}_{\text{G}}$, and a discriminative model $\mathcal{F}_{\text{D}}$, where random noise is transformed by $\mathcal{F}_{\text{G}}$ into a channel sample, and either this generated sample or a true channel sample is accepted by $\mathcal{F}_{\text{D}}$ to produce a real value denoting the probability that the input sample is from the true channel distribution.

[1] In MIMO communication systems, the channel matrices are high-dimensional, and it is in general difficult to characterize an arbitrary high dimensional probability density function [32].

[2] Note that as compared with the reflected channel, the direct channel is much easier to be learned and modeled. Thus, we only focus on the reflected channel modeling problem in this paper due to space limitation.

Note that in the traditional GAN framework, $\mathcal{F}_{\rm D}$ and $\mathcal{F}_{\rm G}$ are usually multi-layer perceptions (MLPs) [22], CNNs [27] or residual networks [28], etc. These networks are trained as black boxes with a large number of training data, and it is difficult to understand their operational mechanisms and investigate how to modify their architectures to achieve better performance. Therefore, we can infer that it would very inefficient to simply adopt these canonical network structures for IRS-related channel modeling since the prior knowledge of the inherent channel property is not exploited. Motivated by this, we embrace the model-driven DL technique [36] in this work and propose to combine it with GAN to solve the considered IRS channel modeling problem. Specifically, the model-driven DL technique [36] is one of the most popular and promising methods for accelerating the training process of neural networks and it has been successfully applied in many other communication problems, such as the LcgNet for massive MIMO detection [37], the LampResNet for mmWave channel estimation [38], and the OFDM-autoencoder [39], etc. Inspired by the model-driven DL technique, we design the network structure in the proposed IRS-GAN framework based on the prior knowledge that the reflected channel is the cascade of the BS-IRS and IRS-user channels.

Since the n-th column of the reflected channel $\mathbf{H}_k$ is the scalar-vector multiplication of the n-th entry of $\mathbf{h}_{r,k}$ and the n-th row of $\mathbf{G}$ (see the reflected channel model given in (3)), we propose a three-node generative model $\mathcal{F}_{\rm G}$ which consists of a BI node $\mathcal{N}_{\rm BI}$, an IU node $\mathcal{N}_{\rm IU}$ and a C node $\mathcal{N}_{\rm C}$, as shown in Fig. 3. First, $\mathcal{N}_{\rm BI}$ is utilized to transform the input random noise vector $\mathbf{z}_{\rm BI}$ from a fixed distribution (usually a uniform or Gaussian distribution) into a matrix $\tilde{\mathbf{G}}$ which approximates the BS-IRS channel $\mathbf{G}$. Note that in a typical CNN, each neuron in the current layer is only connected to a few nearby neurons in the previous layer and the same set of weights is shared by all the neurons in one layer. Based on this weight-sharing architecture and the translational invariance characteristics, CNNs can effectively extract high-level features from the input data. As a result, to approximate the distribution of the BS-IRS channel matrix $\mathbf{G}$ (which is generally high-dimensional and spatially correlated), we treat $\mathbf{G}$ as a two-dimensional natural image and employ a number of two-dimensional convolutional layers, denoted by $\text{CNN}_{\rm BI}(\mathbf{z}_{\rm BI};\boldsymbol{\theta}_{\rm BI})$, to learn the intrinsic correlation among different elements in $\mathbf{G}$, where $\boldsymbol{\theta}_{\rm BI}$ denotes the network parameters included in $\text{CNN}_{\rm BI}(\mathbf{z}_{\rm BI};\boldsymbol{\theta}_{\rm BI})$. Besides, it is noteworthy that a natural BGR image generally consists of three color channels each with real elements, while the wireless channel matrices usually have complex elements. Since most DL platforms require computing with real numbers, we propose to avoid handling complex-valued input channel samples by regarding the real and imaginary parts of $\mathbf{G}$ as two image color channels with real entries. Furthermore, since there is in general a LoS component exists in $\mathbf{G}$ that does not change much over time, an additional bias term $\mathbf{B}_{\rm BI} \in \mathbb{C}^{N\times M}$, is introduced into $\mathcal{N}_{\rm BI}$ to represent this LoS component and $\mathbf{B}_{\rm BI}$ is set to be independent of the input noise vector $\mathbf{z}_{\rm BI}$. Accordingly, the output of $\mathcal{N}_{\rm BI}$, denoted by $\tilde{\mathbf{G}}$, can be expressed as

$$\tilde{\mathbf{G}} = \mathcal{N}_{\rm BI}(\mathbf{z}_{\rm BI};\boldsymbol{\theta}_{\rm BI},\mathbf{B}_{\rm BI}) = \text{CNN}_{\rm BI}(\mathbf{z}_{\rm BI};\boldsymbol{\theta}_{\rm BI}) + \mathbf{B}_{\rm BI}. \quad (5)$$

Second, $\mathcal{N}_{\rm IU}$ is designed to represent the IRS-user channel $\mathbf{h}_{r,k}$ by passing a random noise vector $\mathbf{z}_{\rm IU}$ through a multi-layer fully-connected network $\text{FNN}_{\rm IU}$ and then adding a bias term $\mathbf{b}_{\rm IU} \in \mathbf{C}^{N\times 1}$, i.e.,

$$\tilde{\mathbf{h}}_{r,k} = \mathcal{N}_{\rm IU}(\mathbf{z}_{\rm IU};\boldsymbol{\theta}_{\rm IU},\mathbf{b}_{\rm IU}) = \text{FNN}_{\rm IU}(\mathbf{z}_{\rm IU};\boldsymbol{\theta}_{\rm IU}) + \mathbf{b}_{\rm IU}, \quad (6)$$

where $\tilde{\mathbf{h}}_{r,k}$ denotes the output of $\mathcal{N}_{\rm IU}$ and $\boldsymbol{\theta}_{\rm IU}$ is the learnable parameters included in $\text{FNN}_{\rm IU}$. It is noteworthy that since the IRS-user channel $\mathbf{h}_{r,k}$ is a vector, the FNN structure is employed for simplicity (the CNN structure can also be used in this node). Finally, the node $\mathcal{N}_{\rm C}$ is designed to first concentrate the outputs of $\mathcal{N}_{\rm BI}$ and $\mathcal{N}_{\rm IU}$, then pass these concentrated results through a few fully-connected layers, $\text{FNN}_{\rm C}$, to further approximate the reflected channel and finally output the generated reflected channel samples $\{\tilde{\mathbf{H}}_k\}$, i.e.,

$$\tilde{\mathbf{H}}_k = \mathcal{N}_{\rm C}(\tilde{\mathbf{G}},\tilde{\mathbf{h}}_{r,k};\boldsymbol{\theta}_{\rm C}) = \text{FNN}_{\rm C}\big(f_{\rm CON}(\tilde{\mathbf{G}},\tilde{\mathbf{h}}_{r,k});\boldsymbol{\theta}_{\rm C}\big), \quad (7)$$

where $f_{\rm CON}(\tilde{\mathbf{G}},\tilde{\mathbf{h}}_{r,k}) = \tilde{\mathbf{G}}^H \text{diag}(\tilde{\mathbf{h}}_{r,k})$ and $\boldsymbol{\theta}_{\rm C}$ represents the network parameters of $\text{FNN}_{\rm C}$. Let $\boldsymbol{\Theta}_{\rm G} = \{\boldsymbol{\theta}_{\rm BI},\mathbf{B}_{\rm BI},\boldsymbol{\theta}_{\rm IU},\mathbf{b}_{\rm IU},\boldsymbol{\theta}_{\rm C}\}$ denote the overall learnable parameters in the proposed generative model $\mathcal{F}_{\rm G}$, then we can express $\mathcal{F}_{\rm G}$ based on (5), (6) and (7) as follows:

$$\begin{aligned}\tilde{\mathbf{H}}_k &= \mathcal{F}_{\rm G}(\mathbf{z}_{\rm BI},\mathbf{z}_{\rm IU};\boldsymbol{\Theta}_{\rm G}) \\ &= \text{FNN}_{\rm C}\Big(f_{\rm CON}\big(\text{CNN}_{\rm BI}(\mathbf{z}_{\rm BI};\boldsymbol{\theta}_{\rm BI}) + \mathbf{B}_{\rm BI}, \\ &\qquad \text{FNN}_{\rm IU}(\mathbf{z}_{\rm IU};\boldsymbol{\theta}_{\rm IU}) + \mathbf{b}_{\rm IU}\big);\boldsymbol{\Theta}_{\rm G}\Big). \end{aligned} \quad (8)$$

As for the discriminative model $\mathcal{F}_{\rm D}$, since the reflected channel $\mathbf{H}_k$ can be viewed as a matrix whose columns are scaled versions of those of the BS-IRS channel $\mathbf{G}$ (see (3)) and thereby inherits the spatial correlation in $\mathbf{G}$, we employ a multi-layer CNN, denoted by $\text{CNN}_{\rm D}$, to extract the features in the input channel samples $\{\hat{\mathbf{H}}_k\}$ and determine whether $\hat{\mathbf{H}}_k$ is from the true channel distribution or not. By letting $\boldsymbol{\Theta}_{\rm D}$ denote the network parameters in $\text{CNN}_{\rm D}$, $\mathcal{F}_{\rm D}$ can be represented by

$$\tilde{p}_k = \mathcal{F}_{\rm D}(\hat{\mathbf{H}}_k;\boldsymbol{\Theta}_{\rm D}) = \text{CNN}_{\rm D}(\hat{\mathbf{H}}_k;\boldsymbol{\Theta}_{\rm D}), \quad (9)$$

where the input $\hat{\mathbf{H}}_k$ can be the true channel sample $\mathbf{H}_k$ or the generated channel sample $\tilde{\mathbf{H}}_k$; and the output $\tilde{p}_k$ represents the probability that $\hat{\mathbf{H}}_k$ is drawn from the true channel distribution. To summarize, the proposed IRS-GAN framework is illustrated in Fig. 3.

C. Learning Strategy

In this work, to validate the effectiveness of the proposed IRS-GAN and for simplicity, the training data set is constructed by generating time-independent reflected channel samples according to some known channel models. In practice, we should construct the training data set by collecting the true reflected channel matrices obtained from channel measurements, where the channel estimation methods in [23], [24], [40] can be used. The random noise vectors $\mathbf{z}_{\rm BI}$ and $\mathbf{z}_{\rm IU}$

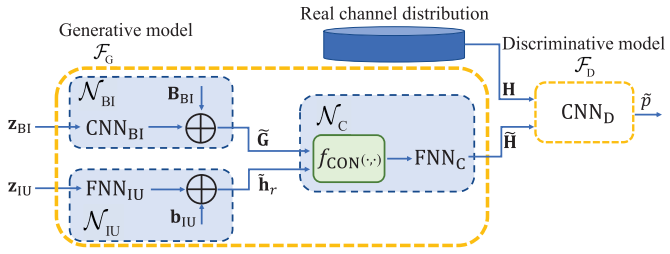

Fig. 3. Proposed IRS-GAN framework.

fed into $\mathcal{F}_{\rm G}$ follow complex normal distributions, i.e., $\mathbf{z}_{\rm BI} \sim \mathcal{CN}(0, \sigma_{z,1}^2\mathbf{I})$ and $\mathbf{z}_{\rm IU} \sim \mathcal{CN}(0, \sigma_{z,2}^2\mathbf{I})$. Besides, the biases in $\mathcal{N}_{\rm BI}$ and $\mathcal{N}_{\rm IU}$, i.e., $\mathbf{B}_{\rm BI}$ and $\mathbf{b}_{\rm IU}$, are randomly generated from $\mathcal{CN}(0, \sigma_{b,1}^2\mathbf{I})$ and $\mathcal{CN}(0, \sigma_{b,2}^2\mathbf{I})$, respectively. The noise variances $\sigma_{z,1}^2$, $\sigma_{z,2}^2$, $\sigma_{b,1}^2$ and $\sigma_{b,2}^2$ are hyper-parameters that determine the initial distribution of the generated channel samples from $\mathcal{F}_{\rm G}$.

Inspired by [27] and [28], we leverage the Wasserstein distance to construct the loss functions for training the generative and discriminative models, which are shown as follows:

$$\mathcal{L}_{\rm G} = \min_{\mathbf{\Theta}_{\rm G}} \mathbb{E}\Big[\max\big\{1 - \mathcal{F}_{\rm D}\big(\mathcal{F}_{\rm G}(\mathbf{z}_{\rm BI}, \mathbf{z}_{\rm IU}; \mathbf{\Theta}_{\rm G}); \mathbf{\Theta}_{\rm D}\big), 0\big\}\Big], \tag{10}$$

$$\mathcal{L}_{\rm D} = \min_{\mathbf{\Theta}_{\rm D}} \mathbb{E}\Big[- \mathcal{F}_{\rm D}(\mathbf{H}_k; \mathbf{\Theta}_{\rm D}) - \max\big\{1 - \mathcal{F}_{\rm D}\big(\mathcal{F}_{\rm G}(\mathbf{z}_{\rm BI}, \mathbf{z}_{\rm IU}; \mathbf{\Theta}_{\rm G}); \mathbf{\Theta}_{\rm D}\big), 0\big\}\Big], \tag{11}$$

where $\mathcal{F}_{\rm D}(\mathbf{H}_k; \mathbf{\Theta}_{\rm D})$ represents the probability that $\mathcal{F}_{\rm D}$ decides that a true channel sample comes from the true channel data set, and $\mathcal{F}_{\rm D}\big(\mathcal{F}_{\rm G}(\mathbf{z}_{\rm BI}, \mathbf{z}_{\rm IU}; \mathbf{\Theta}_{\rm G}); \mathbf{\Theta}_{\rm D}\big)$ denotes the probability that $\mathcal{F}_{\rm D}$ determines that a generated fake channel sample is from the true channel date set; the $\max(\cdot)$ functions in (10) and (11) are introduced to confine the output of $\mathcal{F}_{\rm D}$ to lie in the interval [0,1]. By training $\mathcal{F}_{\rm G}$ and $\mathcal{F}_{\rm D}$ using the loss functions in (10) and (11), $\mathcal{F}_{\rm G}$ and $\mathcal{F}_{\rm D}$ are expected to play a two-player minimax game, i.e., $\min_{\mathbf{\Theta}_{\rm G}} \max_{\mathbf{\Theta}_{\rm D}} \mathbb{E}[\mathcal{F}_{\rm D}(\mathbf{H}_k; \mathbf{\Theta}_{\rm D})] + \mathbb{E}[\max\big\{1 - \mathcal{F}_{\rm D}\big(\mathcal{F}_{\rm G}(\mathbf{z}_{\rm BI}, \mathbf{z}_{\rm IU}; \mathbf{\Theta}_{\rm G}), \mathbf{\Theta}_{\rm D}\big), 0\big\}]$, where $\mathcal{F}_{\rm D}$ is expected to give a high value if the input sample belongs to the true channel data set and a low one if the input is generated by $\mathcal{F}_{\rm G}$, and $\mathcal{F}_{\rm G}$ is trained to fool $\mathcal{F}_{\rm D}$ to output a high probability value when the input is from $\mathcal{F}_{\rm G}$. Since (10) and (11) are based on the Wasserstein distance which is continuous and differentiable everywhere, the proposed IRS-GAN is easier to train and converge as compared to GANs trained with the Jensen-Shannon (JS) divergence based loss function [22], [27].

The training process of the proposed IRS-GAN framework mainly consists of two loops. In each of the outer loop, three inner loops (contains a generative loop, a discriminative loop and a testing loop) are executed sequentially. In the inner generative (discriminative) loop, $\mathcal{F}_{\rm G}$ ($\mathcal{F}_{\rm D}$) is trained with a fixed number of iterations denoted by $I_{\rm G}$ ($I_{\rm D}$). In the testing loop, we calculate a coarse estimate of the Wasserstein distance $\bar{D}_{\rm W} \triangleq \mathbb{E}[\mathcal{F}_{\rm D}(\mathbf{H}_k)] - \mathbb{E}[\mathcal{F}_{\rm D}(\tilde{\mathbf{H}}_k)]$ between the true channel distribution and the generated channel distribution and save it for the next testing loop. Note that $\bar{D}_{\rm W}$ is related with the convergence and the generated sample quality of $\mathcal{F}_{\rm G}$. Let $\alpha_{\rm I}$, $\{\epsilon_1, \epsilon_2\}$ and l denote the initial learning rate, two threshold values, and the outer iteration index, respectively. When $|\bar{D}_{\rm W}^{(l)} - \bar{D}_{\rm W}^{(l-1)}| < \epsilon_1$, the training process is terminated, and if $|\bar{D}_{\rm W}^{(l)} - \bar{D}_{\rm W}^{(l-1)}| \in [\epsilon_1, \epsilon_2]$, the learning rate is set to $\tau\alpha_I$ with τ denoting a decaying factor, otherwise, the next outer loop directly starts with α_I. Note that employing Wasserstein distance based loss functions can effectively improve the stability of learning, but this improvement usually comes at the cost of lower training speed. In this work, to speed up the training procedure, we employ the following three schemes in the proposed learning strategy.

- First, we train $\mathbf{\Theta}_{\rm D}$ by minimizing the sum of $\mathcal{L}_{\rm D}$ and a gradient penalty term $\lambda\mathbb{E}\big[(\|\Delta_{\bar{\mathbf{H}}_k}\mathcal{F}_{\rm D}\ (\bar{\mathbf{H}}_k)\| - 1)^2\big]$, i.e., $\frac{1}{B}\sum_{b=1}^{B}\mathcal{L}_{\rm D,GP}^{(b)}$, where
$$\mathcal{L}_{\rm D,GP}^{(b)} = -\max\big\{1 - \mathcal{F}_{\rm D}(\tilde{\mathbf{H}}_k^{(b)}), 0\big\} - \mathcal{F}_{\rm D}(\mathbf{H}_k^{(b)}) + \lambda\|\nabla_{\bar{\mathbf{H}}_k^{(b)}}\mathcal{F}_{\rm D}(\bar{\mathbf{H}}_k^{(b)})\| - 1)^2, \tag{12}$$
B is batchsize, $\bar{\mathbf{H}}_k = \epsilon\mathbf{H}_k + (1-\epsilon)\tilde{\mathbf{H}}_k$ with $\epsilon \sim U(0,1)$ denoting a random coefficient, and λ is the gradient penalty coefficient which is fixed before training. Note that WGAN sometimes can still generate poor samples or fail to converge, due to the use of weight clipping [27]. Adding this gradient penalty term, which is an alternative to clipping weights, can enable more stable training.
- Second, we propose to add a moment penalty term to $\mathcal{L}_{\rm G}$ such that $\mathcal{F}_{\rm G}$ is forced to focus on learning the statistical information contained in the true channel samples. Specifically, in the generative loop, the corresponding network parameters are learned by minimizing $\frac{1}{B}\sum_{b=1}^{B}\mathcal{L}_{\rm G,MP}^{(b)}$, where
$$\mathcal{L}_{\rm G,MP}^{(b)} = \mu\big(\|\mathbf{H}_k^{(b)}\|_{\rm F} - \|\tilde{\mathbf{H}}_k^{(b)}\|_{\rm F}\big)^2 + \max\big\{1 - \mathcal{F}_{\rm D}(\tilde{\mathbf{H}}_k^{(b)}), 0\big\}, \tag{13}$$
and $\mu\|\mathbb{E}[\mathbf{H}_k^{(b)}] - \mathbb{E}[\tilde{\mathbf{H}}_k^{(b)}]\|_{\rm F}$ represents the moment penalty term with μ denoting the moment penalty coefficient. As such, $\mathcal{F}_{\rm G}$ is expected to produce a distribution that has a similar expectation as the true channel distribution, which is helpful for accelerating the training process especially when the channel has a large deterministic (LoS) component.
- Finally, the initial learning rate for training the bias terms (i.e., $\mathbf{\Theta}_{\rm B} \triangleq \{\mathbf{B}_{\rm BI}, \mathbf{b}_{\rm IU}\}$) is set to be larger than that for training the other network parameters (i.e., $\mathbf{\Theta}_{\rm O} \triangleq \{\boldsymbol{\theta}_{\rm BI}, \boldsymbol{\theta}_{\rm IU}, \boldsymbol{\theta}_{\rm C}\}$ and $\mathbf{\Theta}_{\rm D}$). This modification enables the proposed IRS-GAN to learn the LoS component quickly and then gradually approximate the distribution of the NLoS component.

Besides, all the network parameters in the proposed IRS-GAN are updated by minimizing the corresponding loss functions using the Adam optimizer $\mathrm{Adam}(\cdot, \cdot, \alpha, \beta_1, \beta_2)$, where α is the learning rate, and β_1 and β_2 are the exponential decaying rates for the first and second moment estimates [41].

Note that the proposed channel modeling method can also be extended to IRS-aided MIMO systems where multi-antenna

users are assumed, at the cost of higher network computational complexity. Assuming that each user is equipped with L antennas, the BS-user, BS-IRS and IRS-user channels can be respectively expressed as $\mathbf{H}_d \in \mathbb{C}^{L\times M}$, $\mathbf{G} \in \mathbb{C}^{N\times M}$ and $\mathbf{H}_r \in \mathbb{C}^{L\times N}$. The received signal at the multi-antenna user $\mathbf{y} \in \mathbb{C}^{L\times 1}$ can be written as

$$\mathbf{y} = (\mathbf{H}_r \mathbf{\Theta} \mathbf{G} + \mathbf{H}_d)\mathbf{x} + \mathbf{n}, \tag{14}$$

where $\mathbf{x} \in \mathbb{C}^{M\times 1}$ represents the transmitted signal vector at the BS, $\mathbf{\Theta} \in \mathbb{C}^{N\times N}$ is the reflection pattern, $\mathbf{n} \in \mathbb{C}^{L\times 1}$ denotes the complex Gaussian noise vector. Similar to the single-antenna user case, we can define the reflected channel from the BS to the multi-antenna user via the IRS as

$$\mathbf{H} \triangleq \begin{bmatrix} \text{diag}(\mathbf{H}_{r,1}) & \mathbf{0}_{N\times N} & \cdots & \mathbf{0}_{N\times N} \\ \mathbf{0}_{N\times N} & \text{diag}(\mathbf{H}_{r,2}) & \cdots & \mathbf{0}_{N\times N} \\ \vdots & \vdots & \ddots & \vdots \\ \mathbf{0}_{N\times N} & \mathbf{0}_{N\times N} & \cdots & \text{diag}(\mathbf{H}_{r,L}) \end{bmatrix} \times \left[\mathbf{G}_1^T, \cdots, \mathbf{G}_L^T\right]^T \in \mathbb{C}^{NL\times M}, \tag{15}$$

where $\mathbf{H}_{r,l} \in \mathbf{C}^{1\times N}$ represents the l-th row of $\mathbf{H}_r$, $\mathbf{G}_l = \mathbf{G}, \forall l \in [1, L]$, and $\mathbf{0}_{n\times m}$ represents an $n \times m$ zero matrix. Then, the received signal (14) can be rewritten as

$$\mathbf{y} = (\mathbf{\Theta}_L \mathbf{H} + \mathbf{H}_d)\mathbf{x} + \mathbf{n}, \tag{16}$$

where

$$\mathbf{\Theta}_L \triangleq \begin{bmatrix} \boldsymbol{\theta}^H & \mathbf{0}_{1\times N} & \cdots & \mathbf{0}_{1\times N} \\ \mathbf{0}_{1\times N} & \boldsymbol{\theta}^H & \cdots & \mathbf{0}_{1\times N} \\ \vdots & \vdots & \ddots & \vdots \\ \mathbf{0}_{1\times N} & \mathbf{0}_{1\times N} & \cdots & \boldsymbol{\theta}^H \end{bmatrix} \in \mathbb{C}^{L\times NL}, \tag{17}$$

$\boldsymbol{\theta}$ is the reflection coefficient vector. As can be seen, the proposed channel modeling method can be directly applied to this case and learn the channel distribution of the reflected channel. However, it can be observed that the dimension of the channel matrix in this case is larger and thus the computational complexity would be higher.

IV. IRS-GAN-M for Multiuser System

In this section, we first extend the IRS-GAN framework to the multiuser case and propose an IRS-GAN-M framework that is able to learn the reflected channel distributions associated with different users simultaneously. Then, a multiuser joint learning strategy is presented, after which we theoretically prove the global optimality of the proposed IRS-GAN-M.

A. Proposed IRS-GAN-M

In real communication scenarios, there are in general multiple users. For instance, in a cellular network, multiple users are served by one BS which is roughly located in the center of a cell. Since the wireless channels between the BS and users are usually different due to the different scattering environments, the BS-IRS-user channels need to be modeled independently, which requires a considerably large amount of radio resources and computational complexity. To address this issue, we propose a variant of IRS-GAN for the multiuser case, named as IRS-GAN-M. The foundation of the proposed IRS-GAN-M lies in the fact that each IRS reflecting element reflects the signals from the BS to different users via the same IRS-BS channel. Therefore, according to (3), the reflected channel of an arbitrary user can be regarded as a scaled version of those of the other users. It is thus theoretically feasible to construct a GAN that can learn the reflected channels associated with different users simultaneously with a simplified network structure and reduced number of network parameters, instead of employing multiple identical IRS-GANs independently.

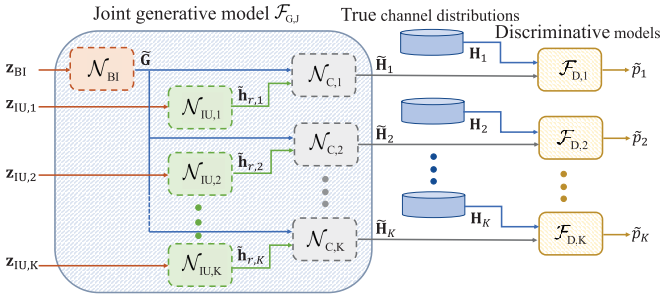

Fig. 4. Proposed IRS-GAN-M.

As shown in Fig. 4, the proposed IRS-GAN-M framework contains one joint generative model $\mathcal{F}_{\text{G,J}}$ and K independent discriminative models $\{\mathcal{F}_{\text{D},1}\}_{k=1}^K$. Inspired by the special structure of $\mathcal{F}_{\text{G}}$ in the single-user case where the channel distributions of the BS-IRS and IRS-user links are learned separately, the proposed $\mathcal{F}_{\text{G,J}}$ in the multiuser case, only needs one BI node $\mathcal{N}_{\text{BI}}$ such that the strong correlation among the reflected channels is blended into the network structure. As a result, we can construct $\mathcal{F}_{\text{G,J}}$ by introducing one BI node $\mathcal{N}_{\text{BI}}$, K IU nodes $\{\mathcal{N}_{\text{IU,k}}\}_{k=1}^K$ and K C nodes $\{\mathcal{N}_{\text{C, k}}\}_{k=1}^K$, then the generated reflected channels associated with different users $\{\tilde{\mathbf{H}}_1, \cdots, \tilde{\mathbf{H}}_K\}$ can be obtained as follows:

$$\{\tilde{\mathbf{H}}_1, \cdots, \tilde{\mathbf{H}}_K\} = \mathcal{F}_{\text{G,J}}\Big(\{\mathbf{z}_{\text{BI}}, \{\mathbf{z}_{\text{IU,k}}\}_{k=1}^K\}; \{\mathbf{\Theta}_{\text{BI}}, \{\mathbf{\Theta}_{\text{IU,k}}\}_{k=1}^K, \{\mathbf{\Theta}_{\text{C,k}}\}_{k=1}^K\}\Big), \tag{18}$$

where $\mathbf{\Theta}_{\text{BI}}$, $\mathbf{\Theta}_{\text{IU,k}} \triangleq \{\boldsymbol{\theta}_{\text{IU,k}}, \mathbf{b}_{\text{IU,k}}\}_{k=1}^K$ and $\mathbf{\Theta}_{\text{C,k}}$ denote the network parameters in $\mathcal{N}_{\text{BI}}$, $\mathcal{N}_{\text{IU,k}}$ and $\mathcal{N}_{\text{C,k}}$, respectively; $\mathbf{z}_{\text{BI}}$ and $\mathbf{z}_{\text{IU}}^k$ denote the noise vectors that are input into the BI node $\mathcal{N}_{\text{BI}}$ and the k-th IU node $\mathcal{N}_{\text{IU,k}}$, respectively. As compared with the naive scheme where K identical IRS-GANs are constructed individually, it can be observed from Fig. 4 that in IRS-GAN-M, $K-1$ redundant BI nodes with the same structure can be removed and hence the number of the network parameters can be substantially reduced. Note that different discriminative models $\{\mathcal{F}_{\text{D,k}}\}_{k=1}^K$ are designed to have the same structure as $\mathcal{F}_{\text{D}}$ in Fig. 3, and they can be expressed as

$$\tilde{p}_k = \mathcal{F}_{\text{D,k}}(\hat{\mathbf{H}}_k; \mathbf{\Theta}_{\text{D,k}}), \quad k \in \mathcal{K}, \tag{19}$$

where $\hat{\mathbf{H}}_k$ represents the input channel samples of $\mathcal{F}_{\text{D,k}}$, which can be a true channel sample, $\mathbf{H}_k$, or a generated channel sample from $\mathcal{F}_{\text{G,J}}$, $\tilde{\mathbf{H}}_k$; $\mathbf{\Theta}_{\text{D,k}}$ denotes the learnable network parameters included in $\mathcal{F}_{\text{D,k}}$.

Furthermore, it is noteworthy that the proposed IRS-GAN-M is very flexible as a variety number of users can be supported without changing the network structure much. In particular, if the reflected channel of an additional user, say U_{K+1}, needs to be modeled, a new IRS-GAN-M can be easily obtained by adding a new IU node and a new C node (i.e., $\mathcal{N}_{\text{IU,K+1}}$ and $\mathcal{N}_{\text{C,K+1}}$) while keeping the previous nodes (i.e., $\{\mathcal{N}_{\text{IU,k}}\}_{k=1}^{K}$ and $\{\mathcal{N}_{\text{C,k}}\}_{k=1}^{K}$) unchanged.

B. Joint Learning Strategy

In this subsection, we present a novel multiuser joint learning strategy for the proposed IRS-GAN-M in the multiuser case, where the joint generative model $\mathcal{F}_{\text{G,J}}$ and K discriminative models $\{\mathcal{F}_{\text{D,k}}\}_{k=1}^{K}$ are able to be trained simultaneously. In other words, all the reflected channels associated with different users can be learned through one complete training process. The details are given as follows.

First, we construct the training data set $\{\mathbf{H}_1^{(i)},\cdots,\mathbf{H}_K^{(i)}\}_{i=1}^{I}$ by generating the reflected channel samples according to a known channel model, where I denotes the size of the training data set. The samples $\{\mathbf{H}_k^{(i)}\}_{i=1}^{I}, k\in\mathcal{K}$ associated with different users are fed then into the corresponding discriminative model $\mathcal{F}_{\text{D,k}}, k\in\mathcal{K}$. In contrast, the joint generative model $\mathcal{F}_{\text{G,J}}$ is trained using the whole training data set $\{\mathbf{H}_1^{(i)},\cdots,\mathbf{H}_K^{(i)}\}_{i=1}^{I}$, thereby the modeled reflected channel associated with each user is based on the knowledge of all users' channels.

Second, for ease of presenting the loss functions for IRS-GAN-M, let us first present the concept of sub-generative models, which are defined as follows:

$$\tilde{\mathbf{H}}_k=\mathcal{F}_{\text{G,J}}^{k}\big(\{\mathbf{z}_{\text{BI}},\mathbf{z}_{\text{IU,k}}\};\{\mathbf{\Theta}_{\text{BI}},\mathbf{\Theta}_{\text{IU,k}},\mathbf{\Theta}_{\text{C,k}}\}\big),\quad k\in\mathcal{K},\tag{20}$$

each of which consists of $\mathcal{N}_{\text{BI}}$, $\mathcal{N}_{\text{IU,k}}$ and $\mathcal{N}_{\text{C,k}}$ and is expected to learn the distribution of the reflected channel associated with U_k. Then, similar to the single-user system, by exploiting the idea of Wasserstein GAN [27], the loss functions for the multiuser case are given as follows:

$$\begin{aligned}\mathcal{L}_{\text{G,J}}=\min_{\mathbf{\Theta}_{\text{G,J}}}\mathbb{E}\Big[\sum_{k\in\mathcal{K}}\max\big\{1-\mathcal{F}_{\text{D,k}}\big(\mathcal{F}_{\text{G,J}}^{k}\big(\{\mathbf{z}_{\text{BI}},\mathbf{z}_{\text{IU,k}}\};\\ \mathbf{\Theta}_{\text{G,J}}^{k}\big);\mathbf{\Theta}_{\text{D,k}}\big),0\big\}\Big],\end{aligned}\tag{21}$$

$$\begin{aligned}\mathcal{L}_{\text{D,k}}=\min_{\mathbf{\Theta}_{\text{D,k}}}\mathbb{E}\Big[-\mathcal{F}_{\text{D,k}}(\mathbf{H}_k;\mathbf{\Theta}_{\text{D,k}})-\max\big\{1\\ -\mathcal{F}_{\text{D,k}}\big(\mathcal{F}_{\text{G,J}}^{k}\big(\{\mathbf{z}_{\text{BI}},\mathbf{z}_{\text{IU,k}}\};\mathbf{\Theta}_{\text{G,J}}^{k}\big);\mathbf{\Theta}_{\text{D,k}}\big),0\big\}\Big],\quad k\in\mathcal{K},\end{aligned}\tag{22}$$

where $\mathbf{\Theta}_{\text{G,J}}^{k}\triangleq\{\mathbf{\Theta}_{\text{BI}},\mathbf{\Theta}_{\text{IU,k}},\mathbf{\Theta}_{\text{C,k}}\}$. It can be observed that $\mathcal{L}_{\text{G,J}}$ maximizes the average outputs of all the discriminative models $\{\mathcal{F}_{\text{D,k}}\}_{k=1}^{K}$ when fed by the generated channel samples, while $\mathcal{L}_{\text{D,k}}$'s are similar to (11).

Finally, similar to the single-user case, the learning strategy in the multiuser case consists of two loops and each outer loop further contains three inner loops, i.e., a discriminative loop, a joint generative loop and a testing loop. In each discriminative loop, the network parameters in $\mathcal{F}_{\text{D,k}}$ are learned by minimizing $\frac{1}{B}\sum_{b=1}^{B}\mathcal{L}_{\text{D,GP,k}}^{(b)}$ where $\mathcal{L}_{\text{D,GP,k}}^{(b)}=-\max\big\{1-\mathcal{F}_{\text{D,k}}(\tilde{\mathbf{H}}_k^{(b)}),0\big\}-\mathcal{F}_{\text{D,k}}(\mathbf{H}_k^{(b)})+\lambda(\|\nabla_{\bar{\mathbf{H}}_k}\mathcal{F}_{\text{D}}(\bar{\mathbf{H}}_k)\|-1)^2$ and $\lambda(\|\nabla_{\bar{\mathbf{H}}_k}\mathcal{F}_{\text{D}}(\bar{\mathbf{H}}_k)\|-1)^2$ represents the gradient penalty term. Note that if a multi-core processor with parallel computing capability is available, the network parameters included in the K discriminative models can be updated in parallel to reduce the training time substantially. In the joint generative loop, the network parameters included in $\mathcal{F}_{\text{G,J}}$ are updated by minimizing the sum of $\mathcal{L}_{\text{G,J}}$ and a moment penalty term, i.e., $\frac{1}{B}\sum_{b=1}^{B}\mathcal{L}_{\text{G,J}}^{(b)}$, where $\mathcal{L}_{\text{G,J}}^{(b)}=\mu\sum_{k\in\mathcal{K}}\mathbb{E}\big[(\|\Delta_{\bar{\mathbf{H}}_k}\mathcal{F}_{\text{D}}(\bar{\mathbf{H}}_k)\|-1)^2\big]+\sum_{k\in\mathcal{K}}\max\big\{1-\mathcal{F}_{\text{D}}(\tilde{\mathbf{H}}_k^{(b)}),0\big\}$. Besides, in the testing loop, we regard the estimated sum Wasserstein distance between the generated channel distributions and the true channel distributions, i.e., $\bar{D}_{\text{W,S}}^{(l)}=\sum_{k\in\mathcal{K}}\Big(\mathbb{E}[\mathcal{F}_{\text{D}}(\mathbf{H}_k)]-\mathbb{E}[\mathcal{F}_{\text{D}}(\tilde{\mathbf{H}}_k)]\Big)$, as the convergence metric of l-th outer iteration. Specifically, if $|\bar{D}_{\text{W,S}}^{(l)}-\bar{D}_{\text{W,S}}^{(l-1)}|<\epsilon_1$, the training process is terminated, if $|\bar{D}_{\text{W,S}}^{(l)}-\bar{D}_{\text{W,S}}^{(l-1)}|\in[\epsilon_1,\epsilon_2]$, the learning rate is set to $\tau\alpha_I$, otherwise, the next outer loop directly starts with α_I.

C. Optimality Analysis

Denote the space of the reflected channel matrices as $\mathcal{H}$, and let $\mathbb{P}_{r,k}$ and $\mathbb{P}_{g,k}, k\in\mathcal{K}$ denote the distributions of the true reflected channels and the randomly generated reflected channel distribution from $\mathcal{F}_{\text{G,J}}$, respectively. In the following, we prove that the minimax game in IRS-GAN-M can achieve a global optimum, i.e., $\mathbb{P}_{r,k}=\mathbb{P}_{g,k},\forall k\in\mathcal{K}$. Note that the analysis is done in a non-parametric setting, and the joint generative model $\mathcal{F}_{\text{G,J}}$ and K discriminative models $\{\mathcal{F}_{\text{D,k}}\}_{k=1}^{K}$ are assumed to have enough capacity.

In the IRS-GAN-M, $\mathcal{F}_{\text{G,J}}$ and $\{\mathcal{F}_{\text{D,k}}\}_{k=1}^{K}$ play a multi-player minimax game with a value function $V\big(\mathcal{F}_{\text{G,J}},\{\mathcal{F}_{\text{D,k}}\}_{k=1}^{K}\big)$, which is shown as follows:

$$\begin{aligned}&\min_{\mathcal{F}_{\text{G,J}}}\max_{\mathcal{F}_{\text{D,1}},\cdots,\mathcal{F}_{\text{D,K}}}V\big(\mathcal{F}_{\text{G,J}},\{\mathcal{F}_{\text{D,k}}\}_{k=1}^{K}\big)\\ &\quad=\sum_{k\in\mathcal{K}}\mathbb{E}_{\mathbf{H}_k\sim\mathbb{P}_{r,k}}[\mathcal{F}_{\text{D,k}}(\mathbf{H}_k)]\\ &\qquad+\sum_{k\in\mathcal{K}}\mathbb{E}_{\mathbf{z}_{\text{BI}}\sim\mathbb{P}_{\text{BI}},\mathbf{z}_{\text{IU,k}}\sim\mathbb{P}_{\text{IU,k}}}\\ &\qquad\times\big[\max\{1-\mathcal{F}_{\text{D,k}}\big(\mathcal{F}_{\text{G,J}}^{k}(\mathbf{z}_{\text{BI}},\mathbf{z}_{\text{IU,k}})\big),0\}\big],\end{aligned}\tag{23}$$

where $\mathbb{P}_{\text{BI}}$ and $\{\mathbb{P}_{\text{IU,k}}\}_{k=1}^{K}$ denote the probability distributions of the noise vectors that are input into $\mathcal{N}_{\text{BI}}$ and $\{\mathcal{N}_{\text{IU,k}}\}_{k=1}^{K}$, respectively. Since $\mathcal{F}_{\text{G,J}}$ can be considered as K generative models that have the same network structure and share some network parameters, $V\big(\mathcal{F}_{\text{G,J}},\{\mathcal{F}_{\text{D,k}}\}_{k=1}^{K}\big)$ can be viewed as the sum of K individual sub-value functions, i.e., $V_k(\mathcal{F}_{\text{G,J}}^{k},\mathcal{F}_{\text{D,k}})=\mathbb{E}_{\mathbf{H}_k\sim\mathbb{P}_{r,k}}[\mathcal{F}_{\text{D,k}}(\mathbf{H}_k)]+\mathbb{E}_{\mathbf{z}_{\text{BI}}\sim\mathbb{P}_{\text{BI}},\mathbf{z}_{\text{IU,k}}\sim\mathbb{P}_{\text{IU,k}}}\big[\max\big\{1-\mathcal{F}_{\text{D,k}}\big(\mathcal{F}_{\text{G,J}}^{k}(\mathbf{z}_{\text{BI}},\mathbf{z}_{\text{IU,k}})\big),0\big\}\big], k\in\mathcal{K}$. As such, the minimax game in (23) can be equivalently transformed into

$$\begin{aligned}&\min_{\mathcal{F}_{\text{G,J}}}\max_{\mathcal{F}_{\text{D,1}},\cdots,\mathcal{F}_{\text{D,K}}}V\big(\mathcal{F}_{\text{G,J}},\{\mathcal{F}_{\text{D,k}}\}_{k=1}^{K}\big)\\ &\quad=\sum_{k\in\mathcal{K}}\min_{\mathcal{F}_{\text{G,J}}}\max_{\mathcal{F}_{\text{D,k}}}V_k(\mathcal{F}_{\text{G,J}}^{k},\mathcal{F}_{\text{D,k}}).\end{aligned}\tag{24}$$

Next, we will show in Lemma 1 and 2 that this minimax game has a global optimum, i.e., $\mathbb{P}_{r,k} = \mathbb{P}_{g,k}, \forall k \in \mathcal{K}$, and in Lemma 3 that the global optimum can be achieved through the proposed learning strategy.

Lemma 1: For a fixed joint generative model $\mathcal{F}_{G,J}$, a set of optimal discriminative models $\{\mathcal{F}^*_{D,1}, \cdots, \mathcal{F}^*_{D,K}\}$ exist.

Proof: Please refer to Appendix A. ■

Lemma 2: The global minimum of the value function V is achieved if and only if $\mathbb{P}_{r,k} = \mathbb{P}_{g,k}, \forall k \in \mathcal{K}$. At that point, V achieves the value K.

Proof: Please refer to Appendix B. ■

Lemma 3: The global minimum of the value function V can be achieved though the joint training strategy.

Proof: Through training, $\mathcal{F}_{\mathrm{D,k}}$'s are able to reach their optimum with fixed $\mathcal{F}_{\mathrm{G,J}}$ at each inner discriminative loop if $\mathcal{F}_{\mathrm{G,J}}$ and $\mathcal{F}_{\mathrm{D,k}}$'s have enough capacity. Then, at the inner generative loop, $\mathbb{P}_{g,k}$'s are updated to minimize the value function V. Note that the subderivatives of the supremum of a convex function include the derivative of this convex function at the point where the maximum is attained [22]. As a result, since the value function $V(\cdot)$ is convex in $\{\mathbb{P}_{g,k}\}_{k=1}^K$ with a unique global optima as shown in Lemma 2, $\mathbb{P}_{g,k} = \mathbb{P}_{r,k}, \forall k \in \mathcal{K}$ can be gradually achieved with sufficient small updates of $\{\mathbb{P}_{g,k}\}_{k=1}^K$. This completes the proof. ■

V. Simulation Results

In this section, we provide numerical results to evaluate the performance of the proposed IRS-GAN and IRS-GAN-M in both single-user and multiuser cases.

A. Experimental Settings

1) System Configuration: We assume a three-dimensional coordinate system where the BS equipped with a uniform linear array (ULA) with M antennas is deployed on the x-axis and the IRS equipped with an $N_y \times N_z$ uniform planar array (UPA) is deployed on the $y-z$ plane. The reference antenna/element at the BS/IRS are located at (2 m, 0, 0) and (0, 45 m, 2 m), respectively. In the simulations, we fix $M = 6$, $N_y = 4$ and $N_z = 8$, respectively. When a large number of IRS elements are deployed, which meets the requirement of Corollary 4 in [42], we can employ the grouping and partition method [43] to achieve a good trade-off between the IRS gain, the channel modeling performance and network complexity. We fix the noise power as $\sigma^2 = -80$ dBm.

2) Performance Metrics: Notice that different from the generative models/networks designed for computer vision tasks (such as those in [22], [27], [44]) whose performance can be directly demonstrated by observing the generated images, it is challenging to evaluate the performance of a generative model/network for the channel modeling problem, especially when the channel matrix is high-dimensional.[3] To address this issue, we design the following metrics in this work.

- Probability distribution function (PDF) of the average singular value of reflected channel matrices: In random matrix theory [45], the average eigenvalue of a random matrix, i.e., the linear eigenvalue statistic, is usually employed to characterize a random square matrix. Inspired by this, we regard the PDF of the average singular value (also referred to as *linear singular value statistics (LSVS)*) as an essential metric to characterize the distribution of the reflected channels.
- Average sum-rates achieved by the two-timescale (TTS) beamforming scheme: The authors in [9] proposed a TTS beamforming optimization scheme for an IRS-aided multiuser system, where the sum-rate maximization problem was solved by using randomly generated channel samples (under the assumption that the BS-user, BS-IRS and IRS-user channel models are perfectly known). Motivated by this, we take the average sum-rate achieved by the TTS beamforming scheme as the second performance metric, where the required channel samples are generated from the trained IRS-GAN, and all the results are averaged over 1000 independent channel realizations.

3) Training Data: In the simulations, due to the difficulty of collecting real channel samples in a practical IRS-aided wireless communication system, we generate the channel samples from some widely-used channel models and a commercial wireless EM propagation software Wireless Insite, and employ the proposed method to learn the corresponding channel distributions. Note that no prior knowledge about the channel models is required by the proposed method, we compare the channel distributions of the generated channel samples from the learned IRS-GAN/IRS-GAN-M and the considered channel models just for validation.

In the literature, spatially correlated Rician fading channel model [46] is one of the most common assumptions in IRS-aided communication systems, e.g., [23] and [24], where both LoS and NLoS components exist. As a result, we first investigate the performance of our method in this channel model, where $\mathbf{h}_{d,k}$, $\mathbf{h}_{r,k}$ and $\mathbf{G}$ can be written as $\mathbf{h}_{d,k} = \sqrt{\frac{\beta^{\mathrm{BU}}}{1+\beta^{\mathrm{BU}}}}\bar{\mathbf{z}}_{d,k} + \sqrt{\frac{1}{1+\beta^{\mathrm{BU}}}}\tilde{\mathbf{z}}_{d,k}$, $\mathbf{h}_{r,k} = \sqrt{\frac{\beta^{\mathrm{IU}}}{1+\beta^{\mathrm{IU}}}}\bar{\mathbf{z}}_{r,k} + \sqrt{\frac{1}{1+\beta^{\mathrm{IU}}}}\tilde{\mathbf{z}}_{r,k}$, $\mathbf{G} = \sqrt{\frac{\beta^{\mathrm{BI}}}{1+\beta^{\mathrm{BI}}}}\bar{\mathbf{F}} + \sqrt{\frac{1}{1+\beta^{\mathrm{BI}}}}\tilde{\mathbf{F}}$. Here β^{BU}, β^{IU} and β^{BI} denote the Rician factors of the BS-user, IRS-user and BS-IRS channels, respectively; $\bar{\mathbf{z}}_{d,k} \in \mathbb{C}^{M\times 1}$, $\bar{\mathbf{z}}_{r,k} \in \mathbb{C}^{N\times 1}$ and $\bar{\mathbf{F}} \in \mathbb{C}^{N\times M}$ represent the LoS components, while $\tilde{\mathbf{z}}_{d,k} \in \mathbb{C}^{M\times 1}$, $\tilde{\mathbf{z}}_{r,k} \in \mathbb{C}^{N\times 1}$ and $\tilde{\mathbf{F}} \in \mathbb{C}^{N\times M}$ represent the corresponding NLoS components. $\tilde{\mathbf{z}}_{d,k}$, $\tilde{\mathbf{z}}_{r,k}$ and $\tilde{\mathbf{F}}$ here are assumed to follow the spatially correlated channel model: $\tilde{\mathbf{z}}_{d,k} = (\mathbf{\Phi}_d)^{\frac{1}{2}}\mathbf{z}_{d,k}$, $\tilde{\mathbf{z}}_{r,k} = \mathbf{\Phi}_{r,k}^{\frac{1}{2}}\mathbf{z}_{r,k}$, $\tilde{\mathbf{F}} = \mathbf{\Phi}_d^{\frac{1}{2}}\mathbf{F}\mathbf{\Phi}_r^{\frac{1}{2}}$, where $[\mathbf{z}_{d,k}]_m \sim \mathcal{CN}\left(0, l^{\mathrm{BU}}_{k,m}\right)$, $[\mathbf{z}_{r,k}]_n \sim \mathcal{CN}\left(0, l^{\mathrm{IU}}_{k,n}\right)$ and $[\mathbf{F}]_{n,m} \sim \mathcal{CN}\left(0, l^{\mathrm{BI}}_{n,m}\right)$ follow the independent and identically distributed (i.i.d.) Rayleigh fading channel model with $^{\mathrm{BU}}_{k,m}$, $l^{\mathrm{IU}}_{k,n}$ and $l^{\mathrm{BI}}_{n,m}$ denoting the distance-dependent path loss of the link from m-th BS antenna to U_k, from the n-th reflecting element to U_k and from the m-th BS antenna to the n-th reflecting element; $l^{\mathrm{BU}}_{k,m} = l_0\left(d_{k,m}/d_0\right)^{-3.4}$, $l^{\mathrm{IU}}_{k,n} = l_0\left(d_{k,n}/d_0\right)^{-3}$ and $l^{\mathrm{BI}}_{m,n} = l_0\left(d_{m,n}/d_0\right)^{-2.2}$, respectively, where $l_0 = -30$ dB represents the path loss at the reference distance $d_0 = 1$ m,

[3]Note that there are several works in the literature (e.g., [19], [21]) that proposed GAN-based channel modeling methods to learn scalar channel responses. In these works, the PDF of the generated channel responses can be employed as the performance metric to assess the proposed modeling methods. However, this metric is not applicable in our work since the reflected channels are two-dimensional matrices.

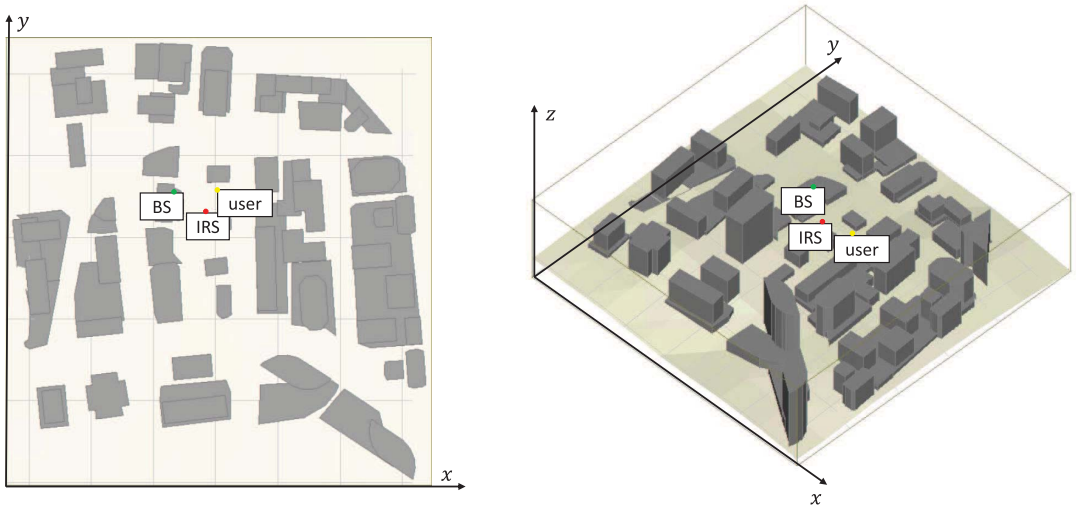

Fig. 5. Simulation setup (a city geometry placed on the terrain).

$d_{k,m}$, $d_{k,n}$ and $d_{m,n}$ denote the link distances. $\mathbf{\Phi}_d$, $\mathbf{\Phi}_r$ and $\mathbf{\Phi}_{r,k}$ represent the BS transmit correlation matrix, the IRS receive correlation matrix and the correlation matrix between the IRS and U_k, respectively. Furthermore, according to [37], [47], the BS transmit correlation matrix can be modeled as

$$\mathbf{\Phi}_d(i,j) = \begin{cases} (r_d)^{j-i}, & \text{if } i \le j, \\ \mathbf{\Phi}_d^*(j,i), & \text{if } i > j, \end{cases} \tag{25}$$

where $r_d \in [0,1]$ is the correlation coefficient. Besides, $\mathbf{\Phi}_r$ ($\mathbf{\Phi}_{r,k}$) can be modeled as $\mathbf{\Phi}_r = \mathbf{\Phi}_r^h \otimes \mathbf{\Phi}_r^v$ ($\mathbf{\Phi}_{r,k} = \mathbf{\Phi}_{r,k}^h \otimes \mathbf{\Phi}_{r,k}^v$) according to [48], where $\mathbf{\Phi}_r^h$ ($\mathbf{\Phi}_{r,k}^h$) and $\mathbf{\Phi}_r^v$ ($\mathbf{\Phi}_{r,k}^v$) denote the spatial correlation matrices of the horizontal and vertical domains, respectively, and they are similarly defined as in (25) with r_r ($r_{r,k}$) denoting the correlation coefficient. Here, we set $r_d = r_{r,k} = 0$ and $r_r = 0.5$.

Second, we also consider a more practical channel model from 3GPP TR 38.901 standard, i.e., the clustered delay line (CDL) model. In the simulations, the CDL-A model is employed for both BS-IRS and IRS-user channels and flat fading is assumed. The resulting cascaded BS-IRS-user channel samples are generated using the Matlab (2019a) 5G Toolbox, where the carrier frequency f_c, sample rate f_s and the maximum doppler shift f_d are set to $f_c = 4$ GHz, $f_s = 1$ MHz and $f_d = 5$ Hz, respectively. The other channel parameters are set according to [49].

Finally, to validate the effectiveness of IRS-GAN in practical communication scenario, we generate channel models from a simulated city communication scenario using the professional wireless propagation software *Wireless Insite*, see Fig. 5. *Wireless Insite* is a professional electromagnetic tool that models the physical characteristics of irregular terrain and urban building features, performs the electromagnetic calculations, and then evaluates the signal propagation characteristics. This can reflect the performance of the proposed method in real IRS-aided communication systems to a certain degree.

4) Training Details: In the following, we introduce the detailed network architecture of the proposed IRS-GAN and the required key hyper-parameters are shown in Table I. For

TABLE I
KEY HYPER-PARAMETERS

Hyper-parameter	Value
Number of true channel samples $\mathbf{H}_k$	50000
Batchsize B	50
Outer iteration number I_O	50
Inner generative iteration number I_G	1000
Inner discriminative iteration number I_D	1000
Gradient penalty coefficient λ	10
Moment penalty coefficient μ	5
Learning rate for training the bias terms α_B	1e-5
Learning rate for training the other parameters α	1e-8
Decaying factor τ	0.1

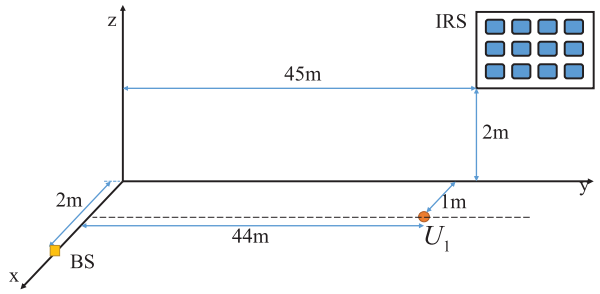

Fig. 6. Simulation setup of the single-user case.

the generative model, CNN_{BI} in the BI node consists of 1 fully-connected input layer, 1 fully-connected output layer and 4 convolutional layers, which produce 256, 128, 64 and 1 feature maps using 5×5, 3×3, 3×3 and 3×3 convolutional cores, respectively, and $\tanh(\cdot)$ is considered as the activation function. Besides, FNN_{IU} and FNN_{C} in the IU and C nodes consist of 3 and 2 fully-connected layers, respectively, where $\tanh(\cdot)$ is also employed as the activation functions. For the discriminative model, CNN_{D} contains 3 convolutional layers, which use the convolutional cores of sizes 5×5, 3×3 and

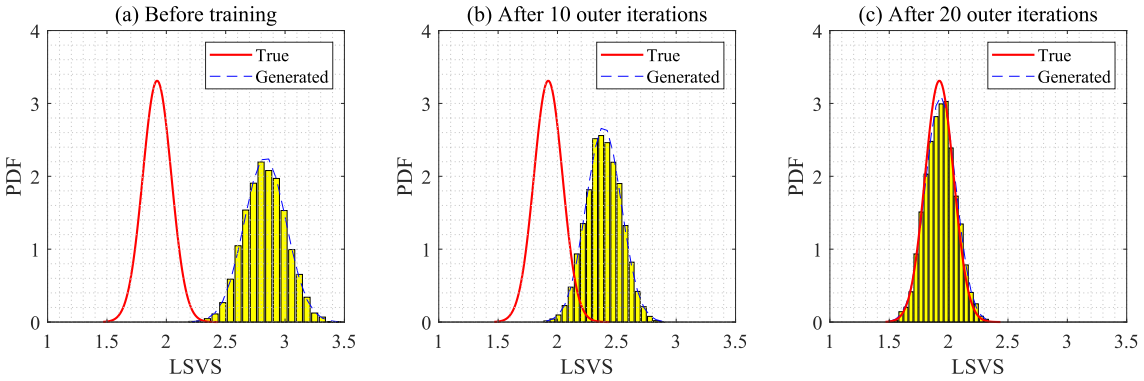

Fig. 7. PDFs of the LSVS of the true reflected channel samples and the generated reflected channel samples by $\mathcal{F}_{\mathrm{G}}$ during the training process.

3×3 to generate 128, 64 and 1 feature maps, and 2 fully-connected output layers. Besides, the ReLU function, i.e., $\mathrm{ReLU}(x) = \max(0, x)$, is served as the activation function. In our simulations, the training process is conducted offline on a Windows server with Intel Xeon Gold 6230 CPU and an Nvidia 2080Ti GPU. The proposed networks are implemented in Python using the TensorFlow library with the Adam optimizer.

B. Single-User Case

In this subsection, we consider the single-user case where the user is set to be located at $(1\ \mathrm{m}, 44\ \mathrm{m}, 0)$, as shown in Fig. 6.

First, we illustrate in Fig. 7 the PDFs of the LSVS of the reflected channel samples generated by $\mathcal{F}_{\mathrm{G}}$ during the training process and compare them with that of the true channel samples. It is can be observed from Fig. 7 (a) that at the beginning of the training process, the LSVS of the generated channel samples is very different from that of the true channel samples due to the random initialization of the proposed IRS-GAN. Then, the proposed network gradually learns to approximate the LSVS of the true channel samples, as can be observed from Fig. 7 (b). After training, the LSVS distributions of the generated channel samples and the true channel samples are almost identical (shown in Fig. 7 (c)), which indicates that the proposed IRS-GAN has successfully learned the reflected channel distribution at least in terms of LSVS. Furthermore, Fig. 8 illustrates the cumulative distribution functions (CDFs) of the LSVS of the generated channel samples in the training process. It is observed that as the number of training iterations increases, the CDF of the LSVS of the generated channel samples gradually converges to that of the true channel and after training for 20 outer iterations, they almost coincide with each other.

Next, we plot in Fig. 9 the average achievable rates achieved by the TTS beamforming scheme [9] based on the true and generated channel samples, under various transmit power budgets. For comparison, we provide the performance achieved by four benchmark methods, including an existing PCA-based channel modeling method [13] and three deep learning based methods, i.e., a CNN-based GAN, an FNN-based GAN and an LSTM-based GAN (abbreviated as CNN-GAN, FNN-GAN and LSTM-GAN in the following), where the conventional CNN, FNN and LSTM are regarded as the generative models, respectively. Specifically, the CNN therein consists of 4 convolution layers, which produce 256, 128, 64 and 1 feature maps using kernels of sizes 5×5, 3×3, 3×3 and 3×3, respectively; the FNN consists of 4 fully-connected layers, which contains $5MN$, $10MN$, $5MN$ and $2MN$ neurons respectively, and $\tanh(\cdot)$ is employed as the activation function of each layer; the LSTM network consists of 3 LSTM layers. First, it can be observed from Fig. 9 that the average achievable rate achieved based on the generated channel samples is almost identical to that achieved based on the true channel samples, and it is higher than those achieved by the CNN-GAN, FNN-GAN and LSTM-GAN. This indicates that the proposed IRS-GAN framework can effectively learn the true reflected channel distribution, and by exploiting the special structure of the reflected channel, IRS-GAN exhibits better performance over other canonical network structures. Second, it can be seen from Fig. 9 (b) that when a more deterministic channel model is considered, the performance gap between the initial GANs and the final converged GANs enlarges. Besides, although the performance of the FNN-GAN/LSTM-GAN are better than (in Fig. 9 (a)) or similar to (in Fig. 9 (b)) that of the CNN-GAN before training, the CNN-GAN outperforms the other two benchmarks after convergence. This is because

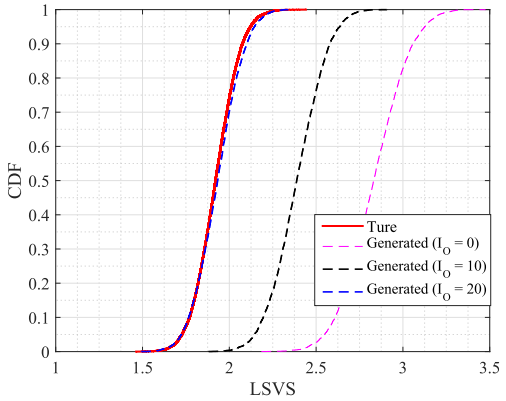

Fig. 8. CDFs of the LSVS of the true reflected channel samples and the generated reflected channel samples by $\mathcal{F}_{\mathrm{G}}$ during the training process.

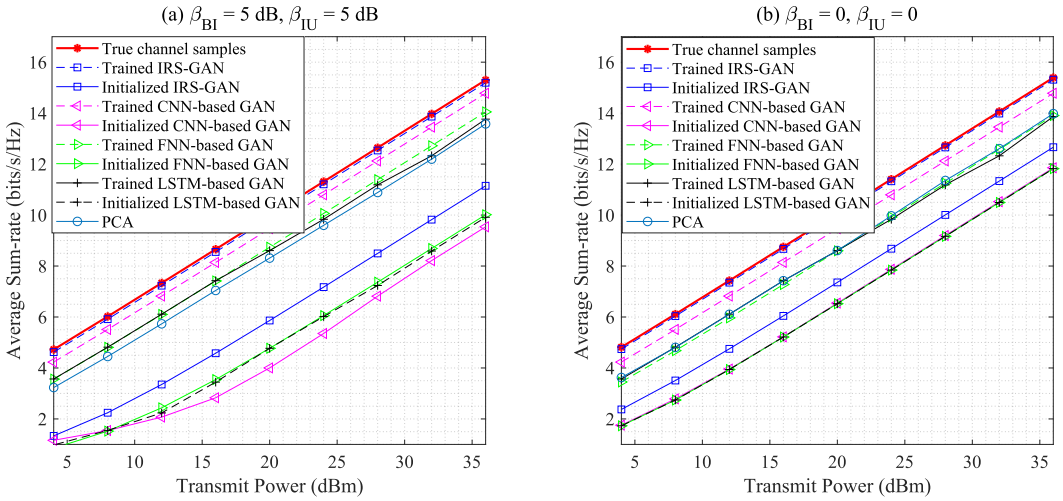

Fig. 9. Average achievable rate performance comparison with different transmit power budgets.

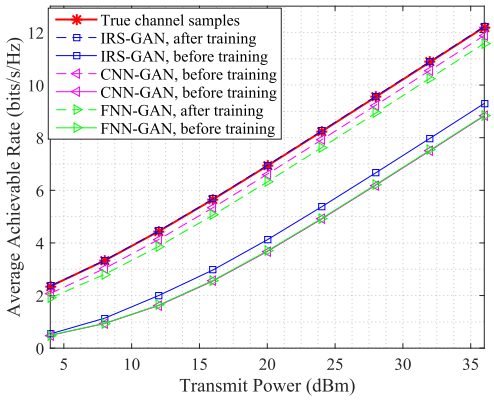

Fig. 10. Average achievable rate performance comparison with different transmit power budgets under the CDL-A channel model.

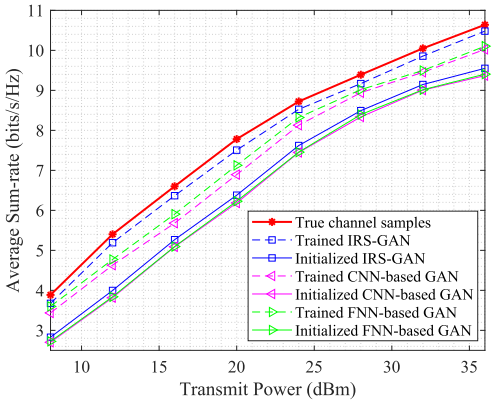

Fig. 11. Average achievable rate performance comparison with different transmit power budgets in the practical scenario.

the convolutional layers are more suitable for extracting high-dimensional features of the input data. As compared to the existing PCA-based method, the proposed IRS-GAN can achieve better performance. This is mainly due to the fact that the proposed IRS-GAN utilizes the property of the reflected channels and exploits the strong power of deep learning, thus it can extract the key features of the underlying channel distributions from the channel samples more accurately. Moreover, different from the PCA-based method, the proposed IRS-GAN can be applied to any other channel models under the same IRS setting, which is more flexible. Although the performance gain is at the expense of high offline training complexity, the online computational complexity of IRS-GAN is limited.

Finally, we investigate the average achievable rate performance in more practical scenarios. First, the results under the 3GPP TR 38.901 CDL-A channel model are shown in Fig. 10. As can be seen, since multi-path time delay and the Doppler effect are considered in the CDL-A channel model, the average achievable rates achieved by the TTS beamforming scheme based on the true or generated channel samples both deteriorate as compared to those under the Rician fading channel model (see Fig. 9). However, the proposed IRS-GAN can still outperform the CNN/FNN-GANs. Furthermore, in Fig. 11, we compare the average achievable rate performance based on the channel data generated by the Wireless InSite Software. The corresponding simulation setup is given in Fig. 5. It is observed from Fig. 11 that the proposed IRS-GAN framework can also effectively learn the reflected

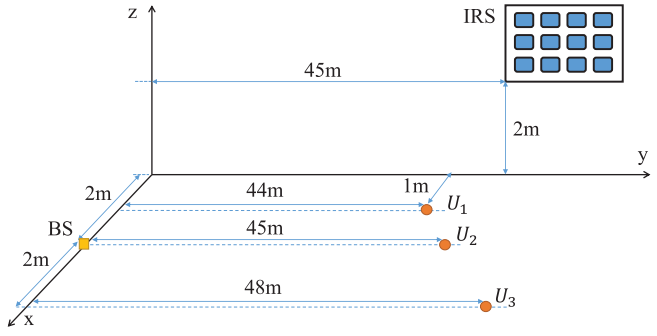

Fig. 12. Simulation setup of the multiuser case.

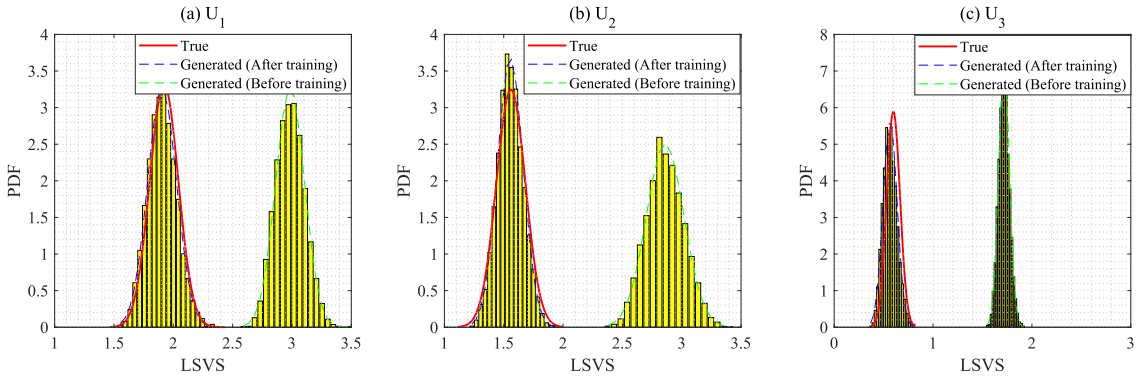

Fig. 13. PDFs of the LSVS of the true reflected channel samples and the generated reflected channel samples by $\mathcal{F}_{\mathrm{G,J}}$ during the training process in the multiuser case.

channel distribution in this practical scenario. Different from the traditional channel modeling methods which are designed for some channel models, the proposed IRS-GAN is more flexible and can be applied to different scenarios through simple finetuning. Therefore, when it is difficult to describe the channel distribution using parameter-based mathematical models, the proposed deep learning based method would be more appealing.

C. Multiuser Case

As shown in Fig. 12, we consider the general multiuser case in this subsection with $K = 3$ and the users are located at $(1\text{ m}, 44\text{ m}, 0)$, $(2\text{ m}, 45\text{ m}, 0)$ and $(4\text{ m}, 48\text{ m}, 0)$, respectively. Without loss of generality, we assume that each IRS-user link has a different correlation level, and the corresponding correlation coefficients are set to $r_{r,k} = \frac{k-1}{3}, \forall k \in \{1, 2, 3\}$.

In Fig. 13, we illustrate the PDFs of the LSVS of the channel samples generated by the initial IRS-GAN-M and trained IRS-GAN-M and compare them with that of the true channel samples. Similar to Fig. 7, it can be observed that at the beginning of the training process, the LSVS of the generated channel samples associated with $U_k, k \in \{1, 2, 3\}$ is very different from that of the true channel sample due to the random initialization of the proposed IRS-GAN-M. After training, the LSVS distributions of the generated channel samples and the true channel samples are almost identical for all the reflected channels.

In Fig. 14, we validate the effectiveness of the proposed IRS-GAN-M and the corresponding joint learning strategy, and the sum-rate performance achieved by the naive scheme (mentioned in Section IV) is also provided for comparison. Specifically, the naive scheme is obtained by constructing K single-user IRS-GANs to learn the channel distributions of the reflected channels associated with K different users and these networks are trained independently. It can be observed from Fig. 14 that the average sum-rates achieved by the IRS-GAN-M (trained with the joint learning strategy) and the independent IRS-GANs (trained with independent learning strategy) are almost identical to that based on the true channel samples. Besides, at the beginning of the training process, one can see that the initial IRS-GAN-M shows a better performance than the initial independent IRS-GANs, this is

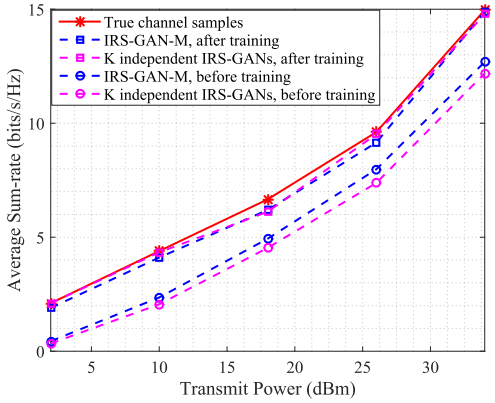

Fig. 14. Average sum-rate performance achieved by the TTS beamforming scheme with different power budgets ($\beta_{\mathrm{BI}} = 5$ dB, $\beta_{\mathrm{IU}} = 5$ dB).

mainly because the correlation among the reflected channels associated with different users is introduced into the design of the IRS-GAN-M.

Furthermore, it is noteworthy that compared with the independent IRS-GANs, the number of network parameters in the proposed IRS-GAN-M can be considerably reduced since the BI node $\mathcal{N}_{\mathrm{BI}}$ is shared by different users. As shown in TABLE II, the time complexity analysis ($M = 6, N = 32, K = 3$) is provided for better illustration, where we measure the time complexity of the proposed method by the number of multiplications. Specifically, the time complexity of a convolutional layer is given by $\mathcal{O}\left(n_{l-1}s_l^2 n_l m_l^2\right)$, where l is the layer index, n_l is the number of filters in the l-th convolutional layer, s_l is the size of the filter, m_l is the spatial size of the output feature map. The time complexity of a fully-connected layer is given by $\mathcal{O}\left(s_{l-1}s_l\right)$ with s_l denoting the number of neurons in the l-th layer. For the generative model, $\mathrm{CNN}_{\mathrm{BI}}$ in the BI node consists of 1 fully-connected input layer, 1 fully-connected output layer and 4 convolutional layers (which produce 256, 128, 64 and 1 feature maps using 5×5, 3×3, 3×3 and 3×3 convolutional cores, respectively). Therefore, the time complexity of $\mathrm{CNN}_{\mathrm{BI}}$ is $C_{\mathrm{BI}} = 2.8892 \times 10^8$. Besides, $\mathrm{FNN}_{\mathrm{IU}}$ and $\mathrm{FNN}_{\mathrm{C}}$ in the IU and C nodes consist of 3 and 2 fully-connected layers, respectively, thus their time complexities are given

TABLE II
TIME COMPLEXITY COMPARISON FOR THE MULTIUSER CASE ($M = 6$, $N = 32$, $K = 3$)

Time Complexity	**IRS-GAN-M**	**Independent IRS-GANs**
Generative model	$C_{\text{BI}} + 3C_{\text{IU}} + 3C_{\text{BU}} = 2.9075 \times 10^8$	$3C_{\text{BI}} + 3C_{\text{IU}} + 3C_{\text{BU}} = 8.6858 \times 10^8$
Discriminative model	$3C_{\text{D}} = 8.9322 \times 10^7$	$3C_{\text{D}} = 8.9322 \times 10^7$
Total	3.8008×10^8	9.5791×10^8

by $C_{\text{IU}} = 22528$ and $C_{\text{C}} = 590208$, respectively. For the discriminative model, CNN_{D} contains 3 convolutional layers, which use the convolutional cores of sizes 5×5, 3×3 and 3×3 to generate 128, 64 and 1 feature maps, and 2 fully-connected output layers, hence the time complexity required is $C_{\text{D}} = 2.9794 \times 10^7$. To summarize, the time complexities of IRS-GAN-M and independent IRS-GANs are listed in TABLE II. We can see that the proposed IRS-GAN-M has much lower time complexity as compared to its counterpart. As such, the training process of the IRS-GAN-M is much simplified. Specifically, in our simulations, the training of the IRS-GAN-M can be completed offline within 1.5 hours, while the training of the IRS-GANs needs about 3.5 hours.

VI. CONCLUSION

In this paper, we studied the channel modeling problem in an IRS-aided MISO system in both single-user and multiuser cases. A model-driven GAN-based channel modeling framework, called IRS-GAN, was proposed to learn the reflected channels, and the proposed framework does not require in-depth domain knowledge in wireless signal propagation and complex data processing. For the single-user case, the special structure of the reflected channel was exploited to design the generative model, which helps to capture the reflected channel distribution effectively. While for the multiuser case, we extended the IRS-GAN framework and proposed an IRS-GAN-M framework, where the multiple distributions of the reflected channels associated with different users are learned simultaneously with reduced number of network parameters. In addition, we theoretically prove that the minimax game in IRS-GAN-M can achieve a global optimum if the generative and discriminative models are given with enough capacity. Finally, extensive simulation results were presented to demonstrate the effectiveness of the proposed IRS-GAN framework for both single-user and multiuser cases.

APPENDIX A
PROOF OF LEMMA 1

According to (24), with fixed $\mathcal{F}_{\text{G,J}}$ (or $\mathcal{F}_{\text{G,J}}^k, k \in \mathcal{K}$), the k-th discriminative model $\mathcal{F}_{\text{D,k}}$ is optimized by maximizing the value function $V_k(\mathcal{F}_{\text{G,J}}^k, \mathcal{F}_{\text{D,k}})$. If $\mathcal{F}_{\text{D,k}}(\cdot) \in [0, 1]$, the value function can be equivalently transformed into

$$\begin{aligned}
&V_k(\mathcal{F}_{\text{G,J}}^k, \mathcal{F}_{\text{D,k}}) \\
&= \mathbb{E}_{\mathbf{H}_k \sim \mathbb{P}_{r,k}}[\mathcal{F}_{\text{D,k}}(\mathbf{H}_k)] \\
&\quad + \mathbb{E}_{\mathbf{z}_{\text{BI}} \sim \mathbb{P}_{\text{BI}}, \mathbf{z}_{\text{IU,k}} \sim \mathbb{P}_{\text{IU,k}}}\big[\max\{1 - \mathcal{F}_{\text{D,k}}\big(\mathcal{F}_{\text{G,J}}^k(\mathbf{z}_{\text{BI}}, \mathbf{z}_{\text{IU,k}})\big), 0\}\big] \\
&= \mathbb{E}_{\mathbf{H}_k \sim \mathbb{P}_{r,k}}[\mathcal{F}_{\text{D,k}}(\mathbf{H}_k)] + \mathbb{E}_{\mathbf{H}_k \sim \mathbb{P}_{g,k}}\big[\max\{1 - \mathcal{F}_{\text{D,k}}(\mathbf{H}_k), 0\}\big] \\
&= 1 + \mathbb{E}_{\mathbf{H}_k \sim \mathbb{P}_{r,k}}[\mathcal{F}_{\text{D,k}}(\mathbf{H}_k)] - \mathbb{E}_{\mathbf{H}_k \sim \mathbb{P}_{g,k}}\big[\mathcal{F}_{\text{D,k}}(\mathbf{H}_k)\big]. \qquad (26)
\end{aligned}$$

By replacing $\mathcal{F}_{\text{D,k}}$ with $\frac{1}{2}\mathcal{F}_{\text{k}} + \frac{1}{2}$ where $\mathcal{F}_{\text{k}} : \mathcal{H} \to [-1, 1]$, we have

$$\begin{aligned}
&\sup_{\mathcal{F}_{\text{D,k}} \in [0,1]} V_k(\mathcal{F}_{\text{G,J}}^k, \mathcal{F}_{\text{D,k}}) \\
&= 1 + \sup_{\mathcal{F}_{\text{D,k}} \in [0,1]} \mathbb{E}_{\mathbf{H}_k \sim \mathbb{P}_{r,k}}[\mathcal{F}_{\text{D,k}}(\mathbf{H}_k)] - \mathbb{E}_{\mathbf{H}_k \sim \mathbb{P}_{g,k}}\big[\mathcal{F}_{\text{D,k}}(\mathbf{H}_k)\big] \\
&= 1 + \frac{1}{2} \sup_{\mathcal{F}_{\text{k}} \in [-1,1]} \mathbb{E}_{\mathbf{H}_k \sim \mathbb{P}_{r,k}}[\mathcal{F}_{\text{k}}(\mathbf{H}_k)] - \mathbb{E}_{\mathbf{H}_k \sim \mathbb{P}_{g,k}}\big[\mathcal{F}_{\text{k}}(\mathbf{H}_k)\big]. \qquad (27)
\end{aligned}$$

Let $\mathcal{X}$ represent an arbitrary compact metric set (such as the space of channel matrices), $\mathbb{P}_1$ and $\mathbb{P}_2$ denote two probability distributions defined on $\mathcal{X}$. Furthermore, let $\|\mathbb{P}_1 - \mathbb{P}_2\|_{\text{TV}}$ represent the total variation (TV) distance between two distributions, which is defined as $\|\mathbb{P}_1 - \mathbb{P}_2\|_{\text{TV}} \triangleq \sup_{A \in \Sigma} |\mathbb{P}_1(A) - \mathbb{P}_2(A)|$, where Σ is the set of all the Borel subsets of $\mathcal{X}$. Note that according to [50], $\sup_{\mathcal{F} \in [-1,1]} \mathbb{E}_{\mathbf{x} \sim \mathbb{P}_1}[\mathcal{F}(\mathbf{x})] - \mathbb{E}_{\mathbf{x} \sim \mathbb{P}_2}\big[\mathcal{F}(\mathbf{x})\big] = \|\mathbb{P}_1 - \mathbb{P}_2\|_{\text{TV}}$ holds, and there exists a function $\mathcal{F}^* : \mathcal{X} \to [-1, 1]$ that satisfies $\mathbb{E}_{\mathbf{x} \sim \mathbb{P}_1}[\mathcal{F}^*(\mathbf{x})] - \mathbb{E}_{\mathbf{x} \sim \mathbb{P}_2}\big[\mathcal{F}^*(\mathbf{x})\big] = \|\mathbb{P}_1 - \mathbb{P}_2\|_{\text{TV}}$. As a result, we have

$$\begin{aligned}
&\sup_{\mathcal{F}_{\text{k}} \in [-1,1]} \mathbb{E}_{\mathbf{H}_k \sim \mathbb{P}_{r,k}}[\mathcal{F}_{\text{k}}(\mathbf{H}_k)] - \mathbb{E}_{\mathbf{H}_k \sim \mathbb{P}_{g,k}}\big[\mathcal{F}_{\text{k}}(\mathbf{H}_k)\big] \\
&\quad = \|\mathbb{P}_{r,k} - \mathbb{P}_{g,k}\|_{\text{TV}}, \quad k \in \mathcal{K}, \qquad (28)
\end{aligned}$$

and there exists an optimal $\mathcal{F}_k^*(\mathbf{H}_k) \in [-1, 1]$ such that the supremum can be achieved. Then, the corresponding optimal discriminative model can be given by $\mathcal{F}_{\text{D,k}}^*(\mathbf{H}_k) = 1 + \frac{1}{2}\mathcal{F}_k^*(\mathbf{H}_k), k \in \mathcal{K}$. This thus completes the proof.

APPENDIX B
PROOF OF LEMMA 2

With the optimal discriminative models $\mathcal{F}_{\text{D,k}}^*(\mathbf{H}_k) = 1 + \frac{1}{2}\mathcal{F}_k^*(\mathbf{H}_k), k \in \mathcal{K}$, the value function in (23) can be written as

$$\begin{aligned}
\min_{\mathcal{F}_{\text{G,J}}} V(\mathcal{F}_{\text{G,J}}, \mathcal{F}_{\text{D,k}}^{*\prime}s) &= \sum_{k \in \mathcal{K}} \min_{\mathcal{F}_{\text{G,J}}} V_k(\mathcal{F}_{\text{G,J}}^k, \mathcal{F}_{\text{D,k}}^*) \\
&= K + \frac{1}{2} \sum_{k \in \mathcal{K}} \|\mathbb{P}_{r,k} - \mathbb{P}_{g,k}\|_{\text{TV}}. \qquad (29)
\end{aligned}$$

Since the TV distance is non-negative, when $\mathbb{P}_{r,k} = \mathbb{P}_{g,k}$, $\|\mathbb{P}_{r,k} - \mathbb{P}_{g,k}\|_{\text{TV}}$ achieves its minimum value 0 and $\min_{\mathcal{F}_{\text{G,J}}^k} V_k(\mathcal{F}_{\text{G,J}}^k, \mathcal{F}_{\text{D,k}}^*) = 1$. As a result, if and only if $\mathbb{P}_{r,k} = \mathbb{P}_{g,k}, \forall k \in \mathcal{K}$, each sub-value function $V_k(\mathcal{F}_{\text{G,J}}^k, \mathcal{F}_{\text{D,k}}^*)$ can reach the value 1, and then the global minimum of $V(\mathcal{F}_{\text{G,J}}, \mathcal{F}_{\text{D,k}}^{*\prime}s)$ (i.e., K) is achieved. This completes the proof.

REFERENCES

[1] Q. Wu and R. Zhang, "Towards smart and reconfigurable environment: Intelligent reflecting surface aided wireless network," *IEEE Commun. Mag.*, vol. 58, no. 1, pp. 106–112, Jan. 2020.

[2] E. Basar, M. Di Renzo, J. De Rosny, M. Debbah, M. Alouini, and R. Zhang, "Wireless communications through reconfigurable intelligent surfaces," *IEEE Access*, vol. 7, pp. 116753–116773, 2019.

[3] Q. Wu *et al.*, "Intelligent reflecting surface aided wireless communications: A tutorial," *IEEE Trans. Commun.*, vol. 69, no. 5, pp. 3313–3351, May 2021.

[4] X. Tan, Z. Sun, D. Koutsonikolas, and J. M. Jornet, "Enabling indoor mobile millimeter-wave networks based on smart reflect-arrays," in *IEEE INFOCOM*, Apr. 2018, pp. 270–278.

[5] M. M. Zhao, Q. Wu, M. J. Zhao, and R. Zhang, "Exploiting amplitude control in intelligent reflecting surface aided wireless communication with imperfect CSI," *IEEE Trans. Commun.*, vol. 69, no. 6, pp. 4216–4231, Jun. 2021.

[6] H. Guo, Y.-C. Liang, J. Chen, and E. G. Larsson, "Weighted sum-rate maximization for reconfigurable intelligent surface aided wireless networks," *IEEE Trans. Wireless Commun.*, vol. 19, no. 5, pp. 3064–3076, May 2020.

[7] C. Huang, A. Zappone, G. C. Alexandropoulos, M. Debbah, and C. Yuen, "Reconfigurable intelligent surfaces for energy efficiency in wireless communication," *IEEE Trans. Wireless Commun.*, vol. 18, no. 8, pp. 4157–4170, Aug. 2019.

[8] Q. Wu and R. Zhang, "Intelligent reflecting surface enhanced wireless network via joint active and passive beamforming," *IEEE Trans. Wireless Commun.*, vol. 18, no. 11, pp. 5394–5409, Nov. 2019.

[9] M.-M. Zhao, Q. Wu, M.-J. Zhao, and R. Zhang, "Intelligent reflecting surface enhanced wireless networks: Two-timescale beamforming optimization," *IEEE Trans. Wireless Commun.*, vol. 20, no. 1, pp. 2–17, Jan. 2021.

[10] M.-M. Zhao, A. Liu, Y. Wan, and R. Zhang, "Two-timescale beamforming optimization for intelligent reflecting surface aided multiuser communication with QoS constraints," *IEEE Trans. Wireless Commun.*, vol. 20, no. 9, pp. 6179–6194, Sep. 2021.

[11] K. Zhi, C. Pan, H. Ren, and K. Wang, "Power scaling law analysis and phase shift optimization of RIS-aided massive MIMO systems with statistical CSI," Oct. 2020, *arXiv:2010.13525*.

[12] Y. Yang *et al.*, "Parallel channel sounder for MIMO channel measurements," *IEEE Wireless Commun.*, vol. 25, no. 5, pp. 16–22, Oct. 2018.

[13] X. Ma, J. Zhang, Y. Zhang, Z. Ma, and Y. Zhang, "A PCA-based modeling method for wireless MIMO channel," in *Proc. IEEE INFOCOM WKSHPS*, May 2017, pp. 874–879.

[14] R. He *et al.*, "Clustering enabled wireless channel modeling using big data algorithms," *IEEE Commun. Mag.*, vol. 56, no. 5, pp. 177–183, May 2018.

[15] P. Petrus, J. H. Reed, and T. S. Rappaport, "Geometrical-based statistical macrocell channel model for mobile environments," *IEEE Trans. Commun.*, vol. 50, no. 3, pp. 495–502, Mar. 2002.

[16] M. Chen *et al.*, "Distributed learning in wireless networks: Recent progress and future challenges," 2021, *arXiv:2104.02151*.

[17] Y. Sun, M. Peng, Y. Zhou, Y. Huang, and S. Mao, "Application of machine learning in wireless networks: Key techniques and open issues," *IEEE Commun. Surveys Tuts.*, vol. 21, no. 4, pp. 3072–3108, 4th Quart., 2019.

[18] L. Bai *et al.*, "Predicting wireless mmWave massive MIMO channel characteristics using machine learning algorithms," *Wireless Commun. Mobile Comput.*, vol. 2018, pp. 1–12, Aug. 2018.

[19] Y. Yang, Y. Li, W. Zhang, F. Qin, P. Zhu, and C.-X. Wang, "Generative-adversarial-network-based wireless channel modeling: Challenges and opportunities," *IEEE Commun. Mag.*, vol. 57, no. 3, pp. 22–27, Mar. 2019.

[20] T. J. Oshea, T. Roy, N. West, and B. C. Hilburn, "Physical layer communications system design over-the-air using adversarial networks," in *Proc. 26th EUSIPCO*, Sep. 2018, pp. 529–532.

[21] H. Ye, L. Liang, G. Y. Li, and B.-H. F. Juang, "Deep learning-based end-to-end wireless communication systems with conditional GANs as unknown channels," *IEEE Trans. Wireless Commun.*, vol. 19, no. 5, pp. 3133–3143, May 2020.

[22] I. J. Goodfellow *et al.*, "Generative adversarial nets," in *Proc. NIPS*, 2014, pp. 1–6.

[23] B. Zheng and R. Zhang, "Intelligent reflecting surface-enhanced OFDM: Channel estimation and reflection optimization," *IEEE Wireless Commun. Lett.*, vol. 9, no. 4, pp. 512–522, Apr. 2020.

[24] Z. Wang, L. Liu, and S. Cui, "Channel estimation for intelligent reflecting surface assisted multiuser communications: Framework, algorithms, and analysis," *IEEE Trans. Wireless Commun.*, vol. 19, no. 10, pp. 6607–6620, Oct. 2020.

[25] H. Jiang, M. Mukherjee, J. Zhou, and J. Lloret, "Channel modeling and characteristics for 6G wireless communications," *IEEE Netw.*, vol. 35, no. 1, pp. 296–303, Jan. 2021.

[26] I. M. Sobol, *A Primer for the Monte Carlo Method*. Boca Raton, FL, USA: CRC Press, 1994.

[27] M. Arjovsky, S. Chintala, and L. Bottou, "Wasserstein GAN," 2017, *arXiv:1701.07875*.

[28] I. Gulrajani, F. Ahmed, M. Arjovsky, V. Dumoulin, and A. Courville, "Improved training of Wasserstein GANs," in *Proc. NIPS*, Dec. 2017, pp. 5767–5777.

[29] X. Yu, V. Jamali, D. Xu, D. W. K. Ng, and R. Schober, "Smart and reconfigurable wireless communications: From IRS modeling to algorithm design," *IEEE Wireless Commun.*, vol. 28, no. 6, pp. 118–125, Dec. 2021.

[30] Y. Han, W. Tang, S. Jin, C.-K. Wen, and X. Ma, "Large intelligent surface-assisted wireless communication exploiting statistical CSI," *IEEE Trans. Veh. Technol.*, vol. 68, no. 8, pp. 8238–8242, Aug. 2019.

[31] Y. Gao, J. Xu, W. Xu, D. W. K. Ng, and M.-S. Alouini, "Distributed IRS with statistical passive beamforming for MISO communications," *IEEE Wireless Commun. Lett.*, vol. 10, no. 2, pp. 221–225, Feb. 2021.

[32] R. M. Neal, "Annealed importance sampling," *Statist. Comput.*, vol. 11, no. 2, pp. 125–139, Apr. 2001.

[33] Y. Bengio, L. Yao, G. Alain, and P. Vincent, "Generalized denoising auto-encoders as generative models," in *Proc. NIPS*, 2013, pp. 1–9.

[34] Y. Bengio, E. Thibodeau-Laufer, and J. Yosinski, "Deep generative stochastic networks trainable by backprop," in *Proc. ICML*, 2014, pp. 226–234.

[35] D. P. Kingma and M. Welling, "Auto-encoding variational Bayes," *CoRR*, vol. abs/1312.6114, pp. 1–14, Dec. 2013.

[36] H. He, S. Jin, C. Wen, F. Gao, G. Y. Li, and Z. Xu, "Model-driven deep learning for physical layer communications," *IEEE Wireless Commun.*, vol. 26, no. 5, pp. 77–83, Oct. 2019.

[37] Y. Wei, M.-M. Zhao, M. Hong, M.-J. Zhao, and M. Lei, "Learned conjugate gradient descent network for massive MIMO detection," *IEEE Trans. Signal Process.*, vol. 68, pp. 6336–6349, 2020.

[38] Y. Wei, M.-M. Zhao, M. Zhao, M. Lei, and Q. Yu, "An AMP-based network with deep residual learning for mmWave beamspace channel estimation," *IEEE Wireless Commun. Lett.*, vol. 8, no. 4, pp. 1289–1292, Aug. 2019.

[39] A. Felix, S. Cammerer, S. Dorner, J. Hoydis, and S. T. Brink, "OFDM-autoencoder for end-to-end learning of communications systems," in *Proc. IEEE SPAWC*, Jun. 2018, pp. 1–5.

[40] Y. Wei, M.-M. Zhao, M.-J. Zhao, and Y. Cai, "Channel estimation for IRS-aided multiuser communications with reduced error propagation," *IEEE Trans. Wireless Commun.*, vol. 21, no. 4, pp. 2725–2741, Apr. 2022.

[41] D. P. Kingma and J. Ba, "Adam: A method for stochastic optimization," in *Proc. Int. Conf. Learn. Represent.*, 2015, pp. 1–15.

[42] M. Najafi, V. Jamali, R. Schober, and H. V. Poor, "Physics-based modeling and scalable optimization of large intelligent reflecting surfaces," *IEEE Trans. Commun.*, vol. 69, no. 4, pp. 2673–2691, Apr. 2021.

[43] C. You, B. Zheng, and R. Zhang, "Channel estimation and passive beamforming for intelligent reflecting surface: Discrete phase shift and progressive refinement," *IEEE J. Sel. Areas Commun.*, vol. 38, no. 11, pp. 2604–2620, Nov. 2020.

[44] A. Radford, L. Metz, and S. Chintala, "Unsupervised representation learning with deep convolutional generative adversarial networks," in *Proc. ICLR*, 2016, pp. 1–16.

[45] G. Livan, M. Novaes, and P. Vivo, *Introduction to Random Matrices: Theory and Practice* (SpringerBriefs in Mathematical Physics). Cham, Switzerland: Springer, 2018.

[46] M. R. McKay and I. B. Collings, "General capacity bounds for spatially correlated Rician MIMO channels," *IEEE Trans. Inf. Theory*, vol. 51, no. 9, pp. 3121–3145, Sep. 2005.

[47] S. L. Loyka, "Channel capacity of MIMO architecture using the exponential correlation matrix," *IEEE Commun. Lett.*, vol. 5, no. 9, pp. 369–371, Sep. 2001.

[48] J. Choi and D. J. Love, "Bounds on eigenvalues of a spatial correlation matrix," *IEEE Commun. Lett.*, vol. 18, no. 8, pp. 1391–1394, Aug. 2014.

[49] *Technical Specification Group Radio Access Network; Study on Channel Model for Frequencies From 0.5 to 100 GHz*, document 3GPP TR 38.901, 2018. [Online]. Available: https://www.3gpp.org/ftp/Specs/archive/38_series/

[50] C. Villani, *Optimal Transport: Old and New*. Berlin, Germany: Springer, 2009.

Yi Wei received the B.Eng. degree in information and communication engineering from Zhejiang University, Hangzhou, China, in 2017, where she is currently pursuing the Ph.D. degree with the College of Information Science and Electronic Engineering. Her research interests include signal processing for wireless communications, algorithm design for advanced MIMO, and deep learning for wireless communications.

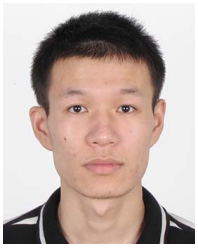

Ming-Min Zhao (Member, IEEE) received the B.Eng. and Ph.D. degrees in information and communication engineering from Zhejiang University, Hangzhou, China, in 2012 and 2017, respectively. From December 2015 to August 2016, he was a Visiting Scholar at the Department of Electrical and Computer Engineering, Iowa State University, Ames, IA, USA. From July 2017 to July 2018, he worked as a Research Engineer at Huawei Technologies Company Ltd. From May 2019 to June 2020, he was a Visiting Scholar at the Department of Electrical and Computer Engineering, National University of Singapore. Since August 2018, he has been working with Zhejiang University, where he is currently an Associate Professor with the College of Information Science and Electronic Engineering. His research interests include channel coding, algorithm design and analysis for advanced MIMO, cooperative communication, and machine learning for wireless communications.

Min-Jian Zhao (Senior Member, IEEE) received the M.Sc. and Ph.D. degrees in communication and information systems from Zhejiang University, Hangzhou, China, in 2000 and 2003, respectively. He was a Visiting Scholar with the University of York, York, U.K., in 2010. He is currently a Professor and the Deputy Director with the College of Information Science and Electronic Engineering, Zhejiang University. His research interests include modulation theory, channel estimation and equalization, MIMO, signal processing for wireless communications, anti-jamming technology for wireless transmission and networking, and communication SOC chip design.